JGR Earth Surface

RESEARCH ARTICLE
10.1029/2019JF005316

Influence of Floods, Tides, and Vegetation on Sediment Retention in Wax Lake Delta, Louisiana, USA

E. A. Olliver[1], D. A. Edmonds[1], and J. B. Shaw[2]

[1]Department of Earth and Atmospheric Science, Indiana University, Bloomington, IN, USA, [2]Department of Geosciences, University of Arkansas, Fayetteville, AR, USA

Key Points:
- Sediment retention analysis on a delta varying riverine flood magnitude, tidal amplitude, and vegetation cover using numerical modeling
- Vertical accretion increases with flood size as input normalized retention decreases, while tides increase retention during large floods
- Vegetation as parameterized reduced accretion and retention due to the greater effect of the buffering effect versus the trapping effect

Supporting Information:
- Supporting Information S1

Correspondence to:
E. A. Olliver,
eolliver@indiana.edu

Citation:
Olliver, E. A., Edmonds, D. A., & Shaw, J. B. (2020). Influence of floods, tides, and vegetation on sediment retention in Wax Lake Delta, Louisiana, USA. *Journal of Geophysical Research: Earth Surface*, *125*, e2019JF005316. https://doi.org/10.1029/2019JF005316

Received 14 AUG 2019
Accepted 19 DEC 2019
Accepted article online 10 JAN 2020
Corrected 4 MAR 2020

This article was corrected on 4 MAR 2020. See the end of the full text for details

Abstract Sediment is the most valuable natural resource for deltaic environments because it is required to build new land. For land building to occur, sediment must be retained in the delta instead of being transported offshore. Despite this, we do not know what controls sediment retention within a delta. Here we use a calibrated numerical model of Wax Lake Delta, Louisiana, USA to analyze sediment retention for different riverine flood magnitudes, tidal amplitudes, and vegetation extents. Our results show that as riverine flood magnitude increases, areally averaged vertical accretion increases from 0.33 to 2 cm per 60-day flood, but sediment retention decreases from 72% to 34%. For the uniform vegetation characteristics considered, the buffering effect, defined as the reduction of sediment flux onto the islands in the presence of vegetation, reduces the sediment flux onto the islands 14 to 22% on a fully vegetated delta. When sediment is transported onto the islands, vegetation enhances retention, which we refer to as the trapping effect, by ~10%. But, this does not offset the buffering effect, and vegetation decreases vertical accretion and retention in the delta up to 6% (or ~0.5 cm per 60-day flood). We suggest that vegetation will increase sedimentation only when trapping compensates for buffering. Finally, greater tidal amplitude at higher discharges enhances vertical accretion by ~0.5 cm per 60-day flood compared to smaller tidal amplitudes. These results provide insight on the mechanisms behind coastal systems growth, and suggest how sediment diversions might be operated more efficiently in deltas with reduced sediment supply.

1. Introduction

Sediment retention is a key unknown in the delta building process. Obviously, sediment must be deposited nearshore for delta building to occur, but we know little about what controls how much of the incoming sediment is retained for delta building and how much is transported out of the delta. The simplest way to quantify retention is as the fraction of sediment deposited relative to the total input over a given time interval (Paola et al., 2011). It is critical that we understand the controls on sediment retention because sediment delivery to most deltas is being reduced. The installation of dams has reduced sediment transport downstream and construction of containment levees has limited the overbank flooding and deposition necessary for wetland sustainment (Blum & Roberts, 2009; Meade & Moody, 2010; Stanley & Warne, 1993; Syvitski et al., 2005; Syvitski & Saito, 2007; Yang et al., 2005). On the Mississippi River Delta, over the past 80 years this sediment starvation, along with compaction and extraction of oil and gas (Jankowski et al., 2017; Kolker et al., 2011), has contributed to the conversion of ~5,000 km^2 of land into open water (Couvillion et al., 2011). Given these losses, it has become widely accepted that coastal restoration in Louisiana must focus on maximizing land building and reducing additional land loss. Despite the reduction in sediment loads to the coast, some river systems still transport enough sediment to build new deltaic wetlands, such as the Atchafalaya and Wax Lake deltas (~135 km southwest of New Orleans, Louisiana at the mouths of the Atchafalaya River and Wax Lake Outlet, respectively) within the greater Mississippi River Delta (MRD; Roberts et al., 2003; Rosen & Xu, 2013; Carle et al., 2015). Thus, a central component of coastal restoration plans in Louisiana is strategic placement and operation of freshwater and sediment diversions, which emulate the natural processes of crevassing and deltaic land building (Coastal Protection and Restoration Authority (CPRA), 2017). Crucially, diverting water and sediment into desired areas does not guarantee land building. Land building will only occur when sediment is retained within the delta, and successful diversions should aim to maximize sediment retention.

Sediment retention depends on the processes that supply and remove sediment in a deltaic system. We divide these processes into continuous or episodic. The continuous processes include riverine discharge,

the presence of vegetation, tides, and waves. Of these continuous processes, field measurements over days to months indicate that riverine discharge is the primary control of sediment delivery to the system, which is important for eventual sediment retention (Allison et al., 2017; Day et al., 2016; Fabre, 2012; Keogh et al., 2019). Previous work has shown that dense vegetation enhances sediment deposition and retention in both salt marshes and deltaic freshwater marshes by decreasing water flow velocities, enhancing bed roughness and shear strength, and directly capturing sediment in the vegetation canopy (Chen et al., 2012; Christiansen et al., 2000; Fagherazzi et al., 2012; Gedan et al., 2011; Larsen, 2019; Leonard & Luther, 1995; Lightbody & Nepf, 2006; Ma et al., 2018; Nepf, 1999; Nepf, 2012a, 2012b; Neumeier & Ciavola, 2004; Tanino & Nepf, 2008; Zong & Nepf, 2010). However, in some instances, vegetation also has been shown to divert flow away from patches of densely vegetated area, resulting in reduced sediment deposition within these patches and increased erosion along their edges due to locally enhanced flow velocities (Chen et al., 2012; Nardin et al., 2016; Nardin & Edmonds, 2014; Nepf, 1999; Nepf, 2012a, 2012b; Piliouras & Kim, 2019; Temmerman et al., 2005, 2007; Van Dijk et al., 2013; Zong & Nepf, 2010).

While we have some sense of how water discharge and vegetation influence retention, relatively little is known about the influence of waves and tides on sediment retention. In the paired observational and numerical modeling study by Allison et al. (2017), they determined from fluorescent tracers that retention of the riverine sediments in the West Bay receiving basin (~7.5 km upstream of the Head of Passes final bifurcation of the Mississippi River channel) was more evenly distributed in space than predicted by the modeling results. Allison et al. (2017) suggested that this more even distribution could be due to influence of tides, waves, or wind-driven currents, which could influence fluid flow in the system and result in changes to the distribution of sediment deposits. However, these forces were not accounted for in the Allison et al. (2017) model. While the microtidal conditions in coastal Louisiana have been shown to have little effect on Mississippi River stages at average and high discharges (Karadogan et al., 2009), it has been suggested that tides may play an important role in regulating water levels and controlling geomorphic evolution in planned sediment diversions that will carry smaller discharges (Hiatt et al., 2019). Tides have been shown to modulate water levels across the Wax Lake Delta (Sendrowski & Passalacqua, 2017), a small developing delta often referred to as a model for diversions (Kim et al., 2009; Paola et al., 2011). Additionally, tides have been observed to influence flow magnitude and direction within at least one deltaic island in the Wax Lake Delta (Hiatt & Passalacqua, 2015) and tidal augmentation of lower discharge flows likely influences reshaping of the subaqueous delta front (Shaw & Mohrig, 2014). The resuspension of sediment by wind-driven waves has been identified as a key process transporting sediment in shallow bays and estuaries in the MRD (Lane et al., 2007; Wang et al., 2018), resulting in sediment transport in and out of deltaic environments. Additionally, edge erosion by waves can result in degradation of existing deltaic marshes (Day et al., 2011; Mariotti, 2016; Ortiz et al., 2017).

While the aforementioned processes are more or less continuously operating, there are also episodic processes, such as hurricanes and seasonal cold fronts that influence sediment retention in the MRD. Southerly and easterly winds of an approaching cold front can result in a net influx of water into coastal bays and wetlands with resulting inundation of 30–50 cm (Childers & Day, 1990; Denes & Caffrey, 1988). Winds shift to westerly and northerly as cold fronts pass, resulting in rapid drainage of the flooded wetlands. The inundation and draining caused by these cold fronts in autumn and winter results in the transport of sediment, nutrients, and organic matter among coastal bays, adjacent wetlands, and the Gulf of Mexico (Childers & Day, 1990; Madden et al., 1988; Perez et al., 2000; Stern et al., 1991). The sediment transport processes associated with cold-front passages have been found to be beneficial for accretion along the eastern portion of the chenier-plain (central and western Louisiana coast), which is directly adjacent to the Atchafalaya system (Draut et al., 2005; Jaramillo et al., 2009; Kineke et al., 2006). However, on Wax Lake Delta, one of the two deltas in the Atchafalaya system, Bevington et al. (2017) showed that during a winter cold front season, sediment was eroded from the deltaic islands. Large storm surges associated with hurricanes occurring between June and November can result in significant deposition and erosion of wetlands (Day et al., 2007; Turner et al., 2006). For example, Hurricanes Katrina and Rita in 2005 resulted in the conversion of ~100 km^2 of wetlands in the Breton Sound Basin (~30 to 35 km downstream of New Orleans, Louisiana along the eastern side of Mississippi River) to shallow marsh with erosion of more than 1 m in some areas, while other areas saw 5–10 cm of deposition (Day et al., 2007). Despite the constructive and destructive force of hurricanes in Breton Sound, Smith et al. (2015) reported long-term sediment

deposition due to hurricanes to be significantly less than what is supplied by fluvial sources. Numerical simulations of Hurricanes Katrina and Rita and their impact on the Wax Lake Delta (WLD) indicate that wave action produced significant erosion (Xing et al., 2017). However, study of elevation change on the deltaic islands of Wax Lake Delta by Bevington et al. (2017) found that Hurricanes Ike and Gustav in 2008 resulted in a net elevation gain on the island tops, while elevation loss was 39% of the gross elevation gain. Additionally, they calculated that the long-term annual contribution of hurricane-derived sediments based on a return period of one every 7–10 years is less than 22% of the sediment delivery by large river floods in the Wax Lake Delta (Bevington et al., 2017).

All of these continuous and episodic processes also vary in time and space, which has an important influence on the meaning of sediment retention. For example, in a study of the West Bay diversion in the MRD, Allison et al. (2017) reported a riverine sand and silt retentions of nearly 100% and 60%, respectively, over two weeks. However, the sand retention rapidly decreased to 40% and the silt retention to 4% after multiple months. Allison et al. (2017) suggest that this decrease in the retention fraction occurred due to flushing of the West Bay basin by rising riverine discharge in the period of time between the initial and final field measurements. Similarly, sediment retention should increase when measured over larger spatial scales, but there is no widely agreed-upon definition of the seaward boundary for a receiving basin (Xu et al., 2019). On the temporal side, the seasonal and intraannual variability of water and sediment discharge strongly influences the magnitude of sediment retention for various years or periods of a given year (Day, Agboola, et al., 2016; Day et al., 2016; Peyronnin et al., 2017). In the Davis Pond Freshwater Diversion (~30 km upstream of New Orleans, Louisiana on the southern side of the Mississippi River), the sediment retention changed from 44% during winter/spring to 81% during summer/fall (Keogh et al., 2019). The lower winter/spring retention fraction likely results from the higher water velocities observed during that period, keeping more sediment in suspension and decreasing water residence over the basin (Keogh et al., 2019). Keogh et al. (2019) also suggested that the seasonally variability in vegetation presence likely contributed to the increase in sediment retention from the winter/spring to summer/fall.

Despite these studies, we still lack an understanding of how these forcing mechanisms interact to retain sediment within a delta. This knowledge gap is of theoretical and practical importance, because understanding how these forces interact would inform how coastal deltaic systems grow and help operate planned sediment diversions more efficiently. Field-based approaches have provided some understanding of relationships between certain forcing mechanisms and sediment retention in a deltaic system, but they have also illustrated just how variable sediment retention can be in time and space (Allison et al., 2017; Day, Agboola, et al., 2016; Esposito et al., 2017; Fabre, 2012; Keogh et al., 2019). A valuable next step would be to study the problem with a numerical model where the data are higher resolution in time and space, and where cause and effect can be more easily isolated. Here we present a calibrated numerical model of Wax Lake Delta built in Delft3D and use it to analyze how sediment retention varies for different flood-wave magnitude, tidal amplitude, and extent of vegetation coverage on the existing deltaic islands. We choose to assess the influence of these three forcing mechanisms because they are continuous in nature, and are either primary drivers for flooding of the deltaic islands or are secondary factors influencing water and sediment transport on and off the islands. We choose to ignore waves in this study because in this portion of the Gulf of Mexico they are small (Georgiou et al., 2005; Wright & Coleman, 1972, 1973), due to the dampening effects of fluid mud nearshore (Kineke et al., 1996; Traykovski et al., 2015). This is obviously a simplification, but Wax Lake Delta is in a relatively protected location within Atchafalaya Bay, making it plausible that waves are a second-order effect. We are interested in how changes in the magnitude of our forcing mechanisms affect sediment retention magnitude and distribution. We calculate the sediment retention for the Wax Lake Delta and assess the spatial distribution of this retained sediment across subsections of the delta (basin, delta front, channels, and islands).

2. Study Area

The WLD is an actively prograding bayhead delta in the Atchafalaya Basin within the greater MRD system. The WLD is located at the mouth of the Wax Lake Outlet (WLO), an artificial diversion of the Atchafalaya River that drains into the Atchafalaya Bay. The Atchafalaya Bay is a shallow, low-energy environment with a

mean wave height of ~0.5 m and mix semidiurnal microtides (average range of ~0.34 m; Rosen & Xu, 2013). The average annual flow in the WLO is 2,500 $m^3 s^{-1}$ and the annual flood tends to peak above 5,000 $m^3 s^{-1}$ (Hiatt & Passalacqua, 2015). The WLO was dredged in 1941 off Six Mile Lake at the downstream end of the Atchafalaya River for flood protection purposes. After 1960, a subaqueous delta began to form at the mouth of the WLO, becoming emergent in 1973 when several deltaic islands were exposed at mean low tide (Robert et al., 1997). WLD experienced rapid growth in the following years due to record flooding in 1973 and 1975 when the average annual sediment load increased from 42.6×10^6 MT in 1965–1972 to 88.8×10^6 MT in 1973–1975 due to flood-induced scouring of the lower reaches of the Atchafalaya River and WLO (Van Heerden & Roberts, 1988). Upon aggrading to an elevation where overlying water was shallow enough, submerged aquatic vegetation established on the highest-elevation portions of the islands. As each island has continued to aggrade, the process of allogenic succession has controlled the development of the heterogeneous freshwater plant community and its distribution on the islands (Cahoon et al., 2011; Carle et al., 2015).

The vegetation community of WLD exhibits sharp community zonation along the elevation gradient of the deltaic islands (Carle et al., 2015). The oldest and highest-elevation portions of the islands, the channel levees, are dominated by black willow (*Salix nigra*) and elephant ear (*Colocasia esculenta*). Intermediate elevations are dominated by dense mixed grasses and forbes, which are clonal in nature and tend to form large monotypic stands (Carle et al., 2015). Emergent forbes like *Sagitarria* species and American lotus (*Nelumbo lutea*) populate periodically exposed mudflats, while floating-leaved (*Potamogeton nodosus*) and submerged aquatic vegetation populate the lowest-elevation portions of the island interiors where water depths remain sufficiently shallow for vegetation colonization (~1 m; Bevington, 2016) and newly formed subaqueous levee deposits (Carle et al., 2015).

As of 2005, ~100 km^2 of new emergent land had been created in WLD (Kim et al., 2009) and the delta continues to grow vertically and laterally (Carle et al., 2015; Kim et al., 2009; Olliver & Edmonds, 2017; Roberts et al., 2003; Rosen & Xu, 2013) in a coastal wetland system with some of the highest land-loss rates in the world (Couvillion et al., 2011; Day et al., 2000; Gagliano et al., 1981). Additionally, WLD has experienced little direct human modification (i.e., dredging or human habitation). Thus, while perhaps an unintended product of the Atchafalaya River diversion, WLD serves as an example of what the diversions proposed in Louisiana's Coastal Protection and Restoration Authority Master Plan hope to accomplish (CPRA, 2017). Its role as a natural field observatory and use as a template in numerical modeling studies can provide insight into how wetlands in these systems develop and what controls sediment retention in them.

3. Methods

3.1. Modeling Domain

To assess the impact of floods, tides, and vegetation on sediment retention within a deltaic system, we constructed a hydrodynamic model of the WLD in Delft3D. Our model of WLD uses a 20-m resolution seamless DEM as the initial bathymetry (Figure 1a). We constructed this DEM using lidar data of the subaerial islands collected as part of the USGS Atchafalaya 2 LiDAR campaign (NOAA, 2011), single-beam bathymetry of the delta front collected in February 2015, and multibeam bathymetry in the distributary channels collected in 2007, 2009, and 2013 (Shaw et al., 2016, their supporting information). The 20-m resolution of our seamless DEM captures the primary channel and island features of the delta, and the smaller channels within the deltaic islands (Figure 1a, inset). Our modeling domain has an upstream boundary where we specify the incoming water discharge and suspended sediment and downstream boundaries where we specify the water-level fluctuations due to tides (Figure 1a). We populate the island tops with vegetation of consistent height (1 m) above the bed surface and uniform spatial density (0.25 m^{-1}), which is calculated assuming ~25 uniformly spaced stems per square meter and a stem diameter of ~1 cm. The stem diameter is typical of *Typha latifolia* (Kadlec & Wallace, 2008), a common species in WLD (Johnson et al., 1985). While our spatial density is lower than the ~40 stems per square meter typical of *T. latifolia* (Grace, 1989; Miller & Fujii, 2010), this density is an intermediate value within the range of tidal freshwater wetland spatial densities considered by Nardin et al. (2016). The interaction between flow and vegetation is governed by the Baptist (2005) formulation. In this study, we use two vegetated extent maps, which represent the areal vegetation coverage at

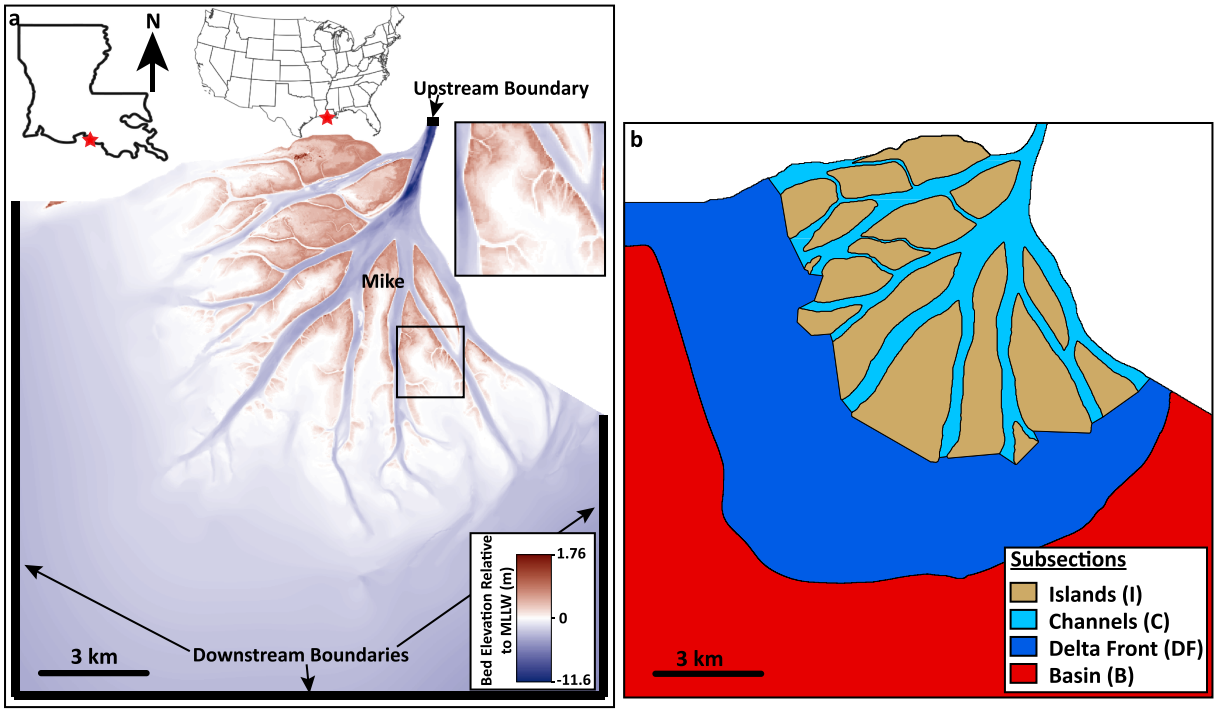

Figure 1. (a) Modeling domain and digital elevation model (DEM) of the Wax Lake Delta, Louisiana, USA. The red star marks the location of Wax Lake Delta along the coast of Louisiana. DEM resolution is 20 m × 20 m and the upstream and downstream model boundaries are marked by bold black lines. The inset image displays how the DEM resolves the primary features of the delta and also the smaller channels in the island interiors. (b) Subsections of the modeling domain used for sediment retention and areally averaged vertical accretion calculations.

minimum and maximum biomass periods of the year, as well as a no vegetation extent map (Figures 2a and 2b). The minimum and maximum vegetated extent maps are based on work presented by Olliver and Edmonds (2017) for the year 2014.

3.2. Model Calibration and Validation

We calibrated our model using field-measured water depths from several platforms located in the interior of Mike Island in WLD (Figures 1a and 3a). For calibration we used water depths from April and September in 2014, representing the minimum and maximum biomass, respectively (Figures 2a and 2b), from three platforms (Figures 3b–3g). The calibration model runs were forced with the water discharge (USGS Calumet gauge on the WLO; Gauge 07381590) and the tidal water levels (NOAA Amerada Pass in the Atchafalaya Delta; Gauge 8764227) over the same time period as the water-depth data were collected. We calibrated the water level in the model to an average root-mean-square error of 0.06 m between the measured and modeled data (Figures 3b–3g). We accomplished this by using different Manning's roughness of $n = 0.01$ for the channels, unvegetated interdistributary bays, and delta front, and an $n = 0.2$ for areas populated by emergent vegetation (dark green area; Figure 2a), and an $n = 0.08$ for the vegetated intertidal zone (light green area; Figure 2b). We also had to raise the downstream tidal water levels by 0.2 m. This suggests that the gauge in Amerada Pass may not faithfully represent the tidal level in neighboring WLD nearly 15 km away. This is not surprising given that the gauge is located within the channel network of the Atchafalaya Delta, and tidal waves are transformed as they funnel through distributary networks and interact with fluvial discharge (Hoitink & Jay, 2016).

To validate the model, we compared model output to measured water depths in 72 locations that were not used in the calibration. From 20 to 23 August 2014, we measured water depths at discrete points (Olliver & Edmonds, 2017; Figure 4a). Using the calibrated model, we ran a simulation over the same time period our water-depth data were collected using upstream water discharge from the USGS Calumet gauge and downstream tidal conditions from Amerada Pass with a 0.2-m increase. We then compared the water depth predicted by the model at the exact time we collected the water-depth data in the field. Our calibrated model

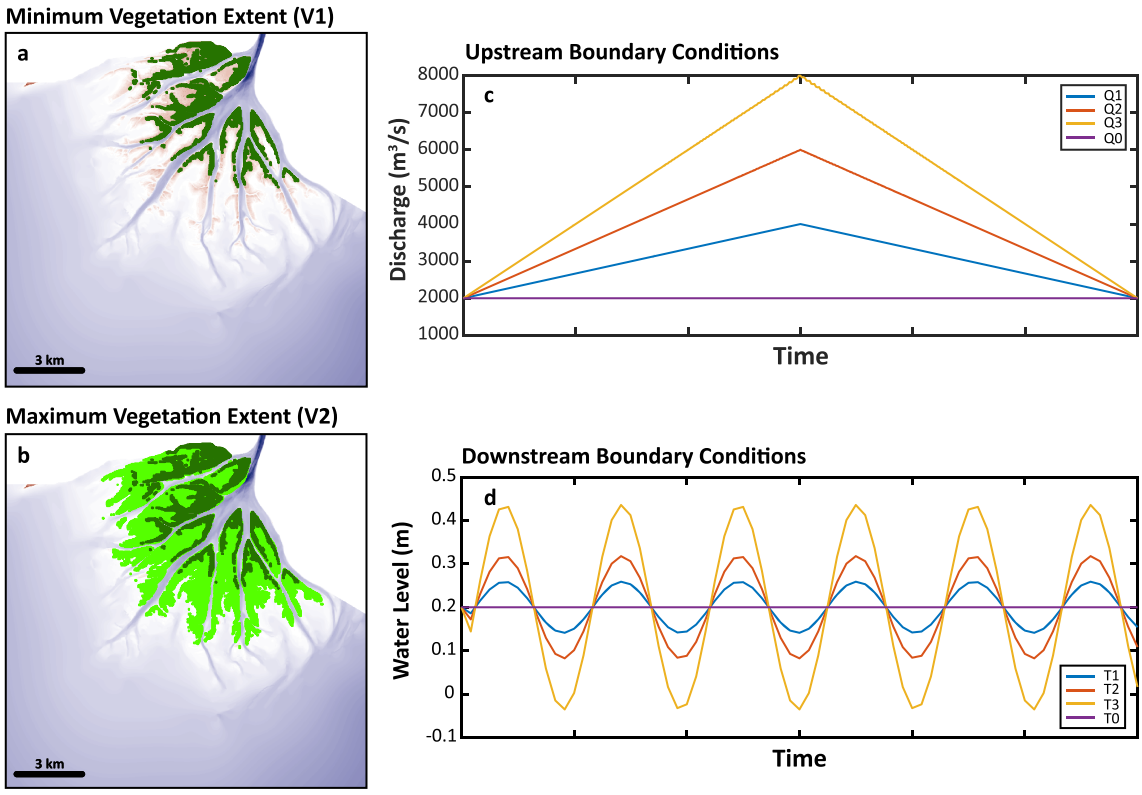

Figure 2. (a and b) The extent of vegetation coverage on the deltaic islands with constant vegetation height (1 m) and density (0.25 m^{-1}) between and throughout for our minimum (V1) and maximum (V2) vegetation extent runs. (c) The riverine floods and (d) tidal amplitudes applied at the upstream and downstream boundary, respectively.

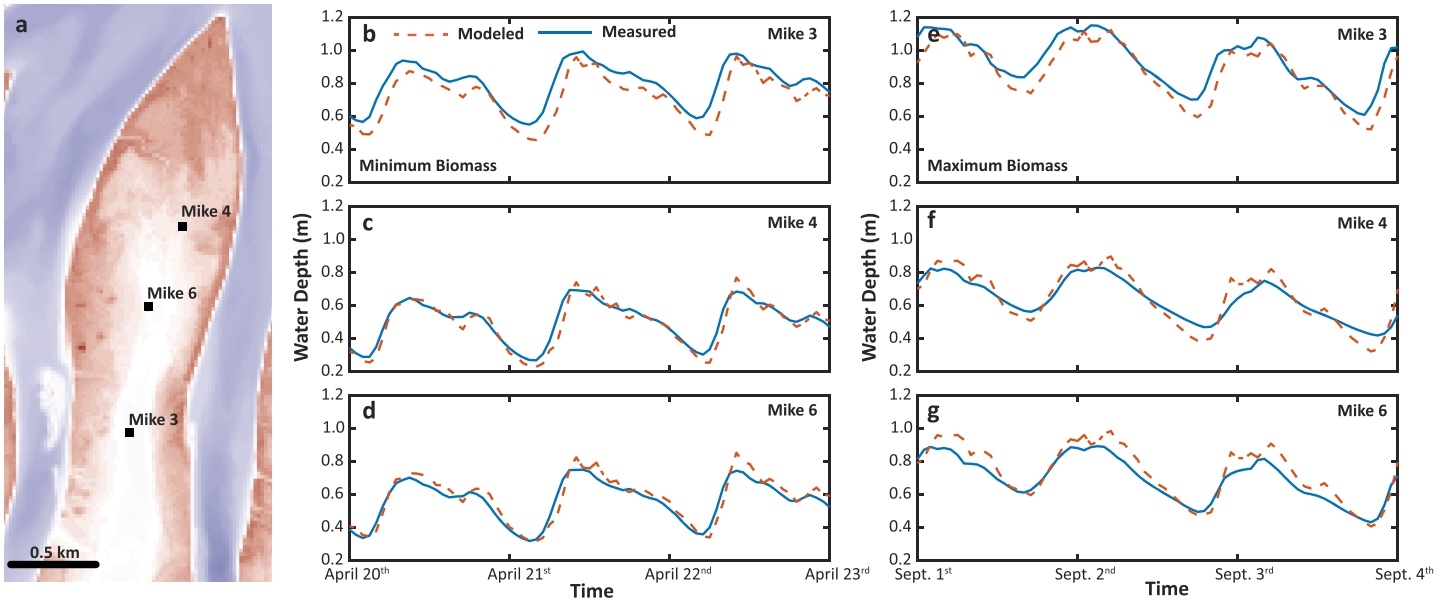

Figure 3. (a) Location of the observation platforms within the interior of Mike Island in WLD (Figure 1a). Model calibration results for (b–d) minimum biomass and (e–g) maximum biomass shows good agreement between observed water-depth data observed (solid line) and modeled (dashed line).

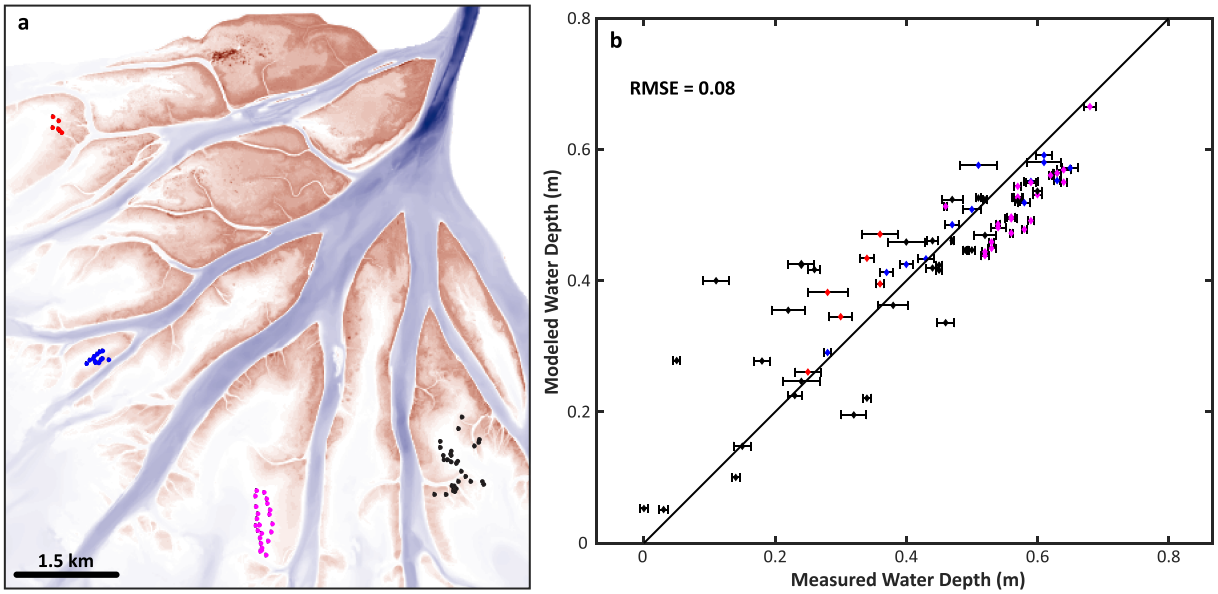

Figure 4. (a) Locations of water depth measurements used for model validation. (b) Measured water depths at locations presented in (a) versus the model-predicted water depths. Solid black line represents a 1:1 fit. Our model accurately predicts water depth to within 8 cm of the observed water depth. The horizontal error bars represent variance of bed elevation within the 20-m cell in which each data point is located as determined using the original 5-m resolution seamless DEM. The data points in (a) and (b) are color coded by island.

predicted water depths with a RMSE = 0.08 m as compared to the observed water-depth data across the deltaic islands (Figure 4).

3.3. Experimental Design and Choice of Boundary Conditions

Our modeling is designed to understand how incoming flood-wave magnitude, tidal amplitude, and the extent of island vegetation coverage affect sediment retention. One approach would be to drive the model with measured hydrographs from the Calumet gauge, and tidal fluctuations from Amerada Pass, but that introduces additional variables that are difficult to control for, such as hydrograph shape or tidal irregularities. Instead, we designed the boundary conditions to be generically representative of these processes. For example, we use a simplified semidiurnal tide in our study runs, even though tides on WLD are actually mix semidiurnal. This simplification was done to reduce the number of interacting tidal variables and allow for smooth variation of the magnitude of tidal amplitude over parameter space, which allows us to more clearly understand cause and effect.

In our model runs the flood-wave magnitude varies over four conditions: a no riverine flood condition but constant discharge of 2,000 $m^3\ s^{-1}$ (*Q0*), to three different triangular floods with a base discharge of 2,000 $m^3\ s^{-1}$ and peak discharges of 4,000 $m^3\ s^{-1}$ (*Q1*), 6,000 $m^3\ s^{-1}$ (*Q2*), and 8,000 $m^3\ s^{-1}$ (*Q3*; Figure 2c). The *Q0* condition is the average base flow during the spring flood period. Our range of peak discharges are an evenly distributed sampling of low-, medium-, and high-magnitude flood discharges based on the range of discharges observed at the USGS Calumet gauge from 1987 to 2018. We simplify the tidal signal to just the semidiurnal component and vary over it four conditions: no tide but constant base level of 0.2 m relative to Mean Lower Low Water (MLLW; *T0*) to three semidiurnal tides with amplitudes of 0.059 m (*T1*), 0.118 m (*T2*), and 0.236 m (*T3*; Figure 2d). The *T0* condition is the water-level adjustment to our downstream boundary made during model calibration. The range of tidal amplitudes for conditions *T1* to *T3* are determined from the range of semidiurnal components measured at the Amerada Pass gauge, which we center on our baseline of 0.2 m relative to MLLW.

The 16 combinations of discharge and tidal conditions were run for three different vegetation conditions for a total of 48 model runs (Table S1). Vegetated extent of the islands varies from a null condition of unvegetated (*V0*) to minimum (*V1*) and maximum vegetated extent (*V2*; Figures 2a and 2b). For *V0*, the alluvial bed roughness is $n = 0.01$ everywhere. For *V1*, the dark green areas (Figure 2a) have $n = 0.2$, and for *V2*, the light green areas have $n = 0.08$ (Figure 2b). All other areas in *V1* and *V2* have $n = 0.01$. Vegetation,

where present, always has a constant height (1 m) and stem density (0.25 m^{-1}). This choice is clearly a simplification because vegetation communities are more complex and are often patchy in space. We ignore the effects of patchiness, even though it can be important (Wright et al., 2018; Yamasaki et al., 2019), because we have little data to constrain the patchy distribution of vegetation at any given time. Also, we do this so we can focus on how vegetation extent of the deltaic islands affects sediment retention. On WLD, the extent of vegetation coverage on the islands varies over the course of the year, due to senescence and removal of much vegetation on the intertidal platform. This significant change in vegetation coverage is likely to alter retention of sediment notably on the delta for the different times of the year. Thus, we choose to consider the end-member conditions of minimum and maximum coverage while keeping height and spatial density of the vegetation within each extent constant between the two vegetation coverage conditions.

We introduce silt (59 μm) and freshwater at the upstream boundary over the duration of the model runs. The basin is assumed to contain freshwater throughout the run. The concentration of suspended silt is set by an empirically derived relationship between discharge and suspended sediment concentration from data collected in the WLO by the USGS (Figure S1). Studies of suspended sediment being delivered to (Shaw et al., 2013) and deposited within the WLD (Shaw & Mohrig, 2014) show that the coarse silt to very fine sand range is the grain size comprising much of the current day deposition on WLD. Sandy deposits comprise roughly two thirds of the WLD (Roberts et al., 1997) and we can reasonably assume that nearly all the sand transported to WLD is deposited somewhere in the delta or its feeder channel. However, data from the USGS gauge at Calumet indicate that ~91% of the sediment entering WLD is silt or finer. Much of this finer load is transported off delta, accumulating on the continental shelf (Allison et al., 2000; Draut et al., 2005; Neill & Allison, 2005), but the significantly greater quantity of fine material in relation to the sand load suggests that future growth and sustainment of WLD is potentially far more sensitive to the transport and accumulation dynamics of silt. These dynamics are weakly understood relative to the dynamics of sand deposition and retention and warrant investigation (Esposito et al., 2017). In addition, since the system is relatively mature, with primary distributary channel levees that inhibit sediment transport onto the islands, the islands are likely nourished primarily by silt that is carried higher in the water column. Thus, we ultimately only consider the silt fraction, selecting a single representative grain size for simplicity.

We set a grain settling velocity of 3 mm s^{-1}. Using Ferguson and Church (2004) this corresponds to a grain size of 59 μm. We define sedimentation as occurring when the grain settling velocity is greater than the turbulent shear velocity. Based on the grain settling velocity, we define the critical bed shear stress for sedimentation as 0.01 N m^{-2}. For simplicity, we eliminate the possibility of erosion or re-suspension of the silt after deposition by setting the critical bed shear stress for erosion at 100 N m^{-2}, although tests for select model runs indicate that this does not change the results (Tables S2 and S3). Delft3D calculates suspended-load transport by solving the diffusion-advection equation. As we use cohesive sediment in our model, the Partheniades-Krone formulations for erosion and deposition were used (Partheniades, 1965). In Delft3D we set our minimum water depth for sediment deposition to 0.1 m. We ran our models for three-day model time, with a morphological scale factor of 20 applied so the runs represent 60 days of bed evolution. This 60-day period represents the median duration of a flood pulse down the WLO based on visual inspection of the Calumet gauge discharge records for the winter/spring flood seasons from 1987 to 2018.

We assessed how the silt moves through the deltaic system by dividing the modeling domain into four subsections based on hydrological and ecogeomorphic attributes: the distributary channel network (C), deltaic islands (I), delta front (DF), and the basin (B; Figure 1b). The boundary between the channel network and island areas is the wet/dry boundary at the bankfull discharge of ~2,000 m^3 s^{-1}. We consider the boundary between each island and the delta front to be the minimally convex hull spanning the two most distal points of vegetated area at maximum biomass. This boundary also roughly coincides with the 0 m relative to MLLW elevation contour. The channel-delta front boundary was defined as a series of minimally convex hulls spanning from the two most distal points of vegetated areas of neighboring islands. Finally, the basin-delta front boundary is set at the −2 m relative to MLLW elevation contour based on work presented by Geleynse et al. (2015).

3.4. Analyses of Model Runs

We calculate four different quantities that describe retention at different scales for our analyses. First, we calculate the porosity-adjusted volume of sediment deposited in each subsection ($D_{subsection}$; m^3) relative to the

total incoming silt measured at the upstream boundary ($Q_{s,o}$; m^3), a term we refer to as delta-scale retention ($F_{\text{subsection}}$):

$$F_{\text{subsection}} = \frac{D_{\text{subsection}}}{Q_{s,0}} \times 100 \quad (1)$$

Delta-scale, in this sense, refers to the total incoming sediment flux at the upstream boundary and subscript *subsection* refers to one of the four subsections in Figure 1b. Second, for only the islands, we calculate the total incoming silt onto the islands ($Q_{s,I}$; m^3) relative to $Q_{s,o}$, a term we refer to as potential delta-scale retention on the islands ($F_{I,P}$):

$$F_{I,P} = \frac{Q_{s,I}}{Q_{s,o}} \times 100 \quad (2)$$

$Q_{s,I}$ is calculated by finding the component of the sediment flux vector perpendicular to the boundary of the island for each model grid cell and summing them all. The difference in $F_{I,P}$ between the unvegetated (V0) and either of the vegetated runs (V1 or V2), for a given set of riverine flood and tidal conditions, quantifies the decrease in sediment flux to the islands due to the presence of vegetation (V1 or V2) as compared to when it is absent (V0):

$$F_{I,P}|_{V0} - F_{I,P}|_{V2} \quad (3)$$

The reduction of sediment influx to the islands in the presence of vegetation as compared to when vegetation is absent is due to the physical reduction or blockage of flow and diversion of flow along the edge of a densely vegetated area. The phenomenon of flow blockage and diversion around a patch of vegetation has been thoroughly studied and is related to the interaction of spatial density of stems, stem diameter, and flow conditions (Chen et al., 2012; Nepf, 1999; Nepf, 2012a, 2012b; Zong & Nepf, 2010), as well as patch size, orientation, and proximity to other patches (Chen et al., 2012; De Lima et al., 2015; Meire et al., 2014; Vandenbruwaene et al., 2011). For the purposes of this study, we refer to the quantified effect of this flow blockage and diversion on sediment influx to the islands ($F_{I,P}|_{V0} - F_{I,P}|_{V2}$) as the buffering effect.

Another term of interest is the difference between the potential ($F_{I,P}$) and actual (F_I) delta-scale retention on the islands for a given set of vegetation and hydrological conditions:

$$F_{I,P} - F_I \quad (4)$$

This quantifies the percentage of silt (relative to the total influx of sediment into the modeling domain, $Q_{s,o}$) that does flow onto the islands, but is not deposited over the course of the run; a term we refer to as silt loss. Fourth, we calculate the total amount of sediment deposited on the islands (D_I; m^3) relative to $Q_{s,I}$, which is the island-scale retention (f_I):

$$f_I = \frac{D_I}{Q_{s,I}} \times 100 \quad (5)$$

The difference in f_I for either the vegetation (V1 or V2) and the unvegetated (V0) run for a given set of riverine flood and tidal conditions quantifies the increase in sediment deposition and retention due to the presence of vegetation as compared to when it is absent:

$$f_I|_{V2} - f_I|_{V0} \quad (6)$$

As our model does not account for direct capture of sediment on the vegetation, enhancement of sediment deposition by vegetation in the case of this study is due to increased drag on sediment laden flow which encourages sediment to fall out of suspension in and around patches of vegetation (Chen et al., 2012; Lightbody & Nepf, 2006; Nepf, 1999; Nepf, 2012a, 2012b; Stumpf, 1983; Tanino & Nepf, 2008; Zong &

Table 1
Delta-Scale Silt Retention ($F_{subsection}$) for V0, V1, and V2 Conditions

	$F_{DF}\|_{V0}$	$F_{DF}\|_{V1}$	$F_{DF}\|_{V2}$	$F_{C}\|_{V0}$	$F_{C}\|_{V1}$	$F_{C}\|_{V2}$	$F_{I}\|_{V0}$	$F_{I}\|_{V1}$	$F_{I}\|_{V2}$	$F_{D}\|_{V0}$	$F_{D}\|_{V1}$	$F_{D}\|_{V2}$	$F_{B}\|_{V0}$	$F_{B}\|_{V1}$	$F_{B}\|_{V2}$	$F_{UD}\|_{V0}$	$F_{UD}\|_{V1}$	$F_{UD}\|_{V2}$
Q0T0	51.82	49.30	48.67	11.82	14.56	14.26	8.80	8.44	3.36	72.44	72.30	66.29	14.90	15.01	15.66	12.66	12.69	18.05
Q0T1	51.63	49.09	48.19	11.91	14.68	14.36	8.45	8.09	3.35	71.99	71.85	65.91	15.13	15.34	17.95	12.87	12.81	16.14
Q0T2	50.47	48.01	46.34	12.27	15.11	14.81	7.74	7.44	3.58	70.48	70.55	64.73	16.03	15.99	19.15	13.49	13.46	16.12
Q0T3	46.84	44.42	42.98	14.01	16.95	16.07	7.01	6.65	4.27	67.85	68.01	63.32	17.19	17.04	19.78	14.96	14.94	16.90
Q1T0	49.40	48.92	42.56	6.07	6.83	7.05	6.23	6.19	3.89	61.70	61.94	53.50	22.14	21.47	25.03	16.16	16.59	21.47
Q1T1	48.40	47.90	42.00	6.05	6.76	6.98	6.28	6.24	3.83	60.73	60.90	52.81	23.58	23.03	26.69	15.69	16.07	20.51
Q1T2	46.48	46.01	41.07	6.24	6.89	7.09	6.11	6.03	3.85	58.84	58.93	52.01	25.55	25.23	28.69	15.61	15.84	19.30
Q1T3	43.30	42.96	39.64	6.97	7.46	7.44	5.84	5.74	4.52	56.10	56.16	51.60	28.37	28.13	30.96	15.53	15.71	17.43
Q2T0	40.34	40.28	34.44	3.94	4.03	4.34	4.09	4.07	3.68	48.38	48.37	42.46	31.48	31.61	31.66	20.14	20.02	25.88
Q2T1	39.81	39.75	34.31	3.91	3.97	4.34	4.25	4.21	3.65	47.97	47.93	42.29	32.62	32.62	33.14	19.41	19.46	24.56
Q2T2	37.88	37.83	33.68	3.98	4.07	4.39	4.52	4.49	3.73	46.38	46.39	41.80	34.35	34.14	33.77	19.27	19.47	24.43
Q2T3	34.96	35.03	32.62	4.39	4.41	4.59	4.70	4.64	4.14	44.05	44.08	41.35	36.61	36.36	35.68	19.34	19.56	22.97
Q3T0	29.65	29.67	27.75	2.66	2.65	3.23	2.94	2.84	3.11	35.24	35.16	34.09	40.24	40.34	33.00	24.52	24.50	32.91
Q3T1	29.06	29.11	27.63	2.68	2.64	3.24	3.04	2.94	3.12	34.78	34.69	34.00	41.27	41.43	34.66	23.95	23.87	31.34
Q3T2	28.38	28.40	27.30	2.71	2.68	3.29	3.32	3.22	3.27	34.41	34.30	33.85	41.87	41.87	35.67	23.73	23.83	30.48
Q3T3	27.21	27.30	26.92	2.96	2.87	3.40	3.72	3.65	3.58	33.89	33.81	33.90	42.34	42.20	37.84	23.77	23.99	28.25

Note. *V0* and *V2* data are shown in Figure 5. D = delta (DF + C + I), DF = delta front, C = delta channels, I = delta islands, B = basin, and UD = undeposited. See Figure 1b for the locations of domains, DF, C, I, and B.

Nepf, 2010). For the purposes of this study, equation (6) embodies vegetation-induced enhancement of sediment deposition, something we refer to as the trapping effect. Finally, we calculate the areally averaged vertical accretion on the islands resulting from the total volume of sediment deposited on the islands (D_I; m^3) by conclusion of the runs ($\overline{\Delta d}_I$; cm):

$$\overline{\Delta d}_I = \frac{D_I}{A_I} \times 100 \tag{7}$$

where A_I (m^2) is the total area of the islands and we multiple the ratio by 100 to convert to cm.

4. Results

The results presented here focus on model runs using the *V0* and *V2* vegetated extents (Figures 2a and 2b). We conducted runs using the *V1* extent, but as we discuss later, these results are nearly identical to *V0* (Table 1). Here we focus on how retention varies at the delta-scale and as a function of the hydrodynamic drivers of river discharge, and tidal amplitude. The effects of vegetation are discussed in the sections of river discharge and tidal amplitude.

4.1. Delta-Scale Retention

As flood-wave magnitude increases, the percentage of the total silt input retained in the delta as a whole ($F_D = F_I + F_C + F_{DF}$) decreases from 72 to 34% without vegetation (V0) and from 66 to 34% with vegetation (V2; Figure 5 and Table 1; $F_D|_{V0}$ and $F_D|_{V2}$ progressing from *Q0* to *Q3* across all *T* conditions). Progressing from *Q0* to *Q3* across all *T* and *V* conditions, the majority of sediment retained within the delta is deposited in the delta front (52 to 27%), followed by the channels (14 to 3%), and islands (8 to 3%; Figure 5 and Table 1; F_{DF}, F_C, and F_I, respectively). This decrease in retention occurs because at higher Q_w the higher flow velocities cause sediment to bypass the delta topset. As a result, silt retention in the basin (F_B) increases with *Q* from 15 to 42% (*V0*) and 16 to 38% (*V2*). The proportion of $Q_{s,o}$ that exits the domain at the downstream boundary or remains in suspension when the run ends (F_{UD}) also increases from 13 to 24% (*V0*) and 18 to 28% (*V2*) with increasing Q_w (Figure 5 and Table 1).

As tidal amplitude increases (*T0* to *T3*) retention in the delta as a whole (F_D) decreases by 3 to 5% for *Q0*, but only decreases retention by ~1.5% for *Q3* (Table 1; F_D progressing from *T0* to *T3* for *Q0* and *Q3*, respectively). This trend of reducing retention on the delta is mostly due to the consistent decrease in retention on the delta front with increasing tidal amplitude across all *Q* and V conditions (Table 1; F_{DF} always decreases progressing from *T0* to *T3* for a given *Q* and *V* condition). Interestingly,

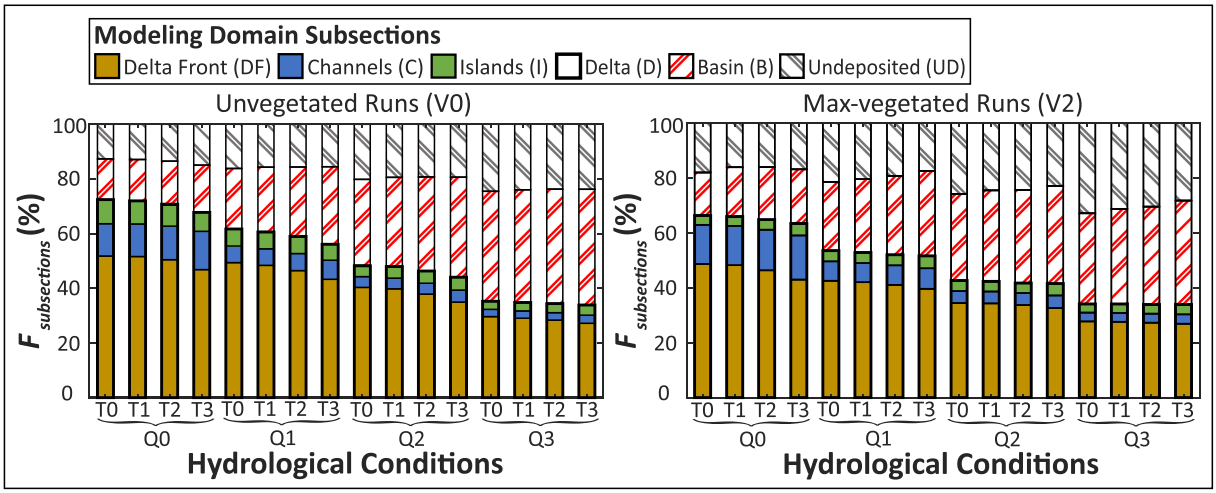

Figure 5. Delta-scale silt retention (F) for each modeling domain subsection for each of our (a) unvegetated ($V0$) and (b) max-vegetated ($V2$) runs. Along the x axis, each grouping of four is a riverine flood condition ($Q0$–3), with each bar in a grouping a tidal condition ($T0$–3). On the y axis, the bars are divided into the proportional amounts of $Q_{s,o}$ for each given run retained in each domain subsection. The undeposited subsection represents the proportion of $Q_{s,o}$ that has exited the domain or remains in suspension at run conclusion.

retention in the channels (F_C) and islands (F_I) has a more variable response and increases or decreases with increasing tidal amplitude at different Q and V conditions (Table 1; F_C and F_I do not always decrease progressing from $T0$ to $T3$).

The presence of vegetation reduces F_D by as much as ~6% for $Q0$ and ~0.5% for $Q3$ (Table 1; $F_D|_{V0}$ versus $F_D|_{V2}$ for all of $Q0$ and $Q3$, respectively). Specifically, the presence of vegetation decreases retention in the delta front (DF) and islands (I) by 1 to 4% and 0.5 to 5%, respectively, while retention in the channels (C) increases by 0.5 to 3% (Table 1; $F_{DF,I,C}|_{V0}$ versus $F_{DF,I,C}|_{V2}$ across all Q and T conditions). Conversely, vegetation increases retention in the basin (B) from 1 to 5%, as well as the proportion of $Q_{s,o}$ that remains undeposited (from 2 to 8%; Table 1; $F_{B\ and\ UD}|_{V0}$ versus $F_{B\ and\ UD}|_{V2}$ across all Q and T conditions).

Surprisingly, there is almost no difference in retention for the $V0$ and $V1$ condition across our runs (Table 1; F_{V0} versus F_{V1} across all Q and T conditions). This suggests to us that, as least for the model simplifications and range of parameters considered in this study, the minimal vegetation condition behaves like a completely unvegetated delta.

4.2. The Role of Flood-Wave Magnitude

The amount of sediment that flows onto the deltaic islands is a quantity of interest as the deltaic islands make up the subaerial landscape, and to keep pace with relative sea-level rise they must be nourished by sediment. $F_{I,P}$ is the proportion of $Q_{s,o}$ that flows onto the islands and is the maximum potential sediment retention on the islands (equation (2)). The difference between the potential retention for the $V0$ and the $V2$ conditions ($F_{I,P}|_{V0} - F_{I,P}|_{V2}$, ; equation (3)) qualifies how vegetation alters sediment influx to the islands, something we call the buffering effect (Figure 6; length of dashed gray arrow denotes magnitude of buffering effect). Then, the difference between incoming sediment and deposited sediment ($F_{I,P} - F_I$; equation (4)) is the percentage of silt (relative to $Q_{s,o}$) that does flow onto the islands but is not deposited, something we term silt loss (Figure 6; length of dashed black arrow denotes magnitude of silt loss). The $F_{I,P}$ and F_I results cluster according to flood-wave magnitude and vegetated extent, and each cluster contains four points that correspond to different tidal amplitudes (Figure 6; $F_{I,P}$ and F_I clusters outlined by dashed and solid lines, respectively).

First, we consider how the amount of sediment that flows onto the islands as a function of what is coming into the delta ($F_{I,P}$) changes as a function of discharge. Not surprisingly, as Q_w increases, so do $F_{I,P}$ and $\overline{\Delta d}_I$ for both the $V0$ and $V2$ runs because larger floods transport more sediment onto the islands. However, the $V2$ runs have lower $\overline{\Delta d}_I$, and much lower $F_{I,P}$, compared to $V0$. This occurs because the magnitude of the buffering effect ($F_{I,P}|_{V0} - F_{I,P}|_{V2}$) changes as a function of discharge. Thus, at $Q0$ the buffering effect reduces $F_{I,P}$ by

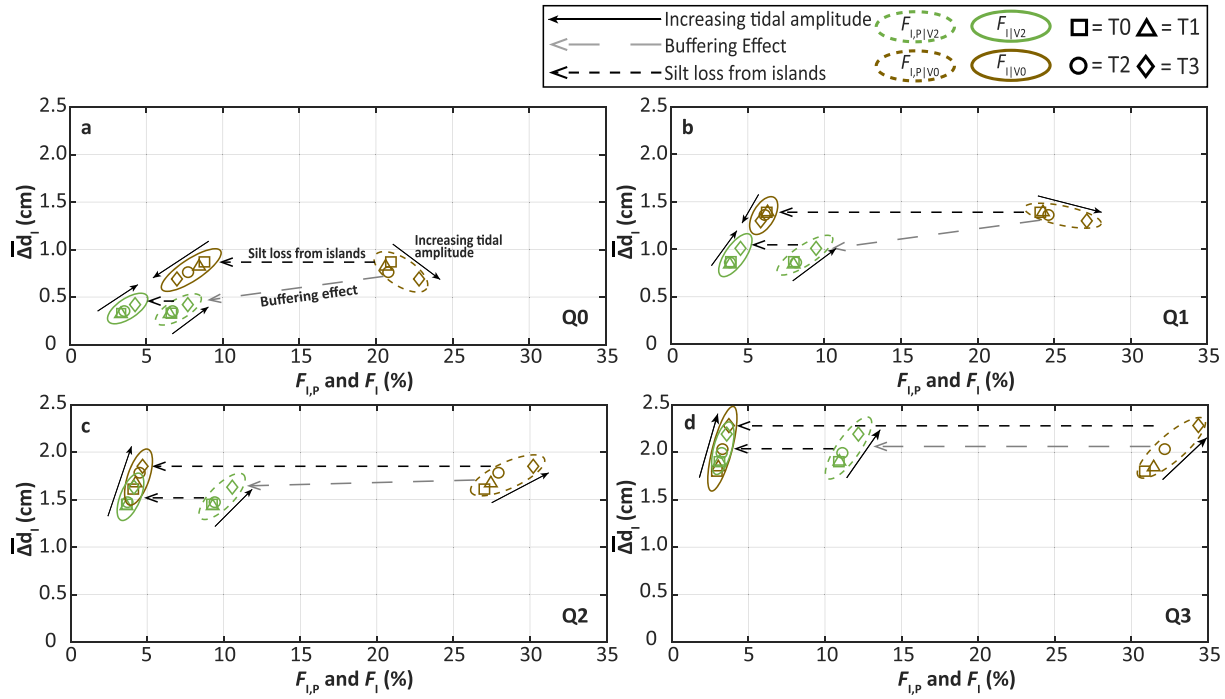

Figure 6. (a–d) The relationship between sediment retention and accretion on the islands at the delta-scale. We present the data for each riverine flood condition (*Q0–3*) in a separate plot for clarity. The data clusters in each plot consist of the four tidal amplitude conditions (*T0–3*) for a set of riverine flood and vegetation conditions and are outlined by dashed and solid lines for the $F_{I,P}$ and F_I data, respectively. The brown or green color of the cluster outlines denotes the *V0* and *V2* condition, respectively. The dashed gray arrow between the $F_{I,P}|_{V0}$ and $F_{I,P}|_{V2}$ data clusters denotes the buffering effect. The dashed black arrows between the $F_{I,P}$ and F_I data clusters for a given vegetation condition denote the loss of silt from the islands. The solid black arrows alongside each $F_{I,P}$ and F_I grouping highlight the trend of increasing tidal amplitude.

roughly 14%, whereas at *Q3* the buffering effect reduces $F_{I,P}$ by about 20% (Figure 6 and Table 2). If we view the buffering effect proportionally then $\frac{Q_{s,I}|_{V2}}{Q_{s,I}|_{V0}} \approx 67\%$ for nearly all runs. The consistency of this proportion is likely because we do not vary vegetation parameters, such as height and density, among our runs.

Table 2
Average Vertical Accretion, and Delta-Scale (F) and Island-Scale (f) Sediment Retention for the V0 and V2 Conditions

	$F_{I,P}\|_{V0}$	$F_{I,P}\|_{V2}$	Buffering effect $F_{I,P}\|_{V0} - F_{I,P}\|_{V2}$	$F_I\|_{V0}$	$F_I\|_{V2}$	Silt loss from islands $F_{I,P}\|_{V0} - F_I\|_{V0}$	Silt loss from islands $F_{I,P}\|_{V2} - F_I\|_{V2}$	$f_I\|_{V0}$	$f_I\|_{V2}$	$\overline{\Delta d}_I\|_{V0}$	$\overline{\Delta d}_I\|_{V2}$
Q0T0	20.98	6.64	14.33	8.80	3.36	12.18	3.28	41.95	50.65	0.87	0.33
Q0T1	20.63	6.52	14.11	8.45	3.35	12.18	3.17	40.97	51.35	0.83	0.33
Q0T2	20.82	6.73	14.09	7.74	3.58	13.08	3.15	37.19	53.18	0.76	0.35
Q0T3	22.81	7.72	15.10	7.01	4.27	15.80	3.45	30.70	55.38	0.69	0.42
Q1T0	24.09	8.00	16.09	6.23	3.89	17.86	4.11	25.87	48.60	1.39	0.87
Q1T1	24.27	7.99	16.28	6.28	3.83	17.99	4.16	25.89	47.90	1.40	0.85
Q1T2	24.64	8.15	16.48	6.11	3.85	18.53	4.30	24.81	47.18	1.36	0.86
Q1T3	27.13	9.45	17.67	5.84	4.52	21.29	4.93	21.51	47.79	1.30	1.01
Q2T0	27.02	9.24	17.79	4.09	3.68	22.93	5.56	15.15	39.81	1.61	1.45
Q2T1	27.44	9.28	18.16	4.25	3.65	23.19	5.63	15.50	39.28	1.68	1.44
Q2T2	27.95	9.43	18.53	4.52	3.73	23.43	5.70	16.17	39.55	1.78	1.47
Q2T3	30.21	10.56	19.65	4.70	4.14	25.51	6.42	15.57	39.22	1.85	1.63
Q3T0	30.88	10.91	19.98	2.94	3.11	27.94	7.80	9.52	28.51	1.80	1.90
Q3T1	31.46	10.94	20.52	3.04	3.12	28.42	7.82	9.65	28.56	1.85	1.91
Q3T2	32.20	11.15	21.05	3.32	3.27	28.88	7.88	10.30	29.30	2.03	1.99
Q3T3	34.38	12.18	22.20	3.72	3.58	30.66	8.60	10.83	29.42	2.28	2.19

Note. These data are plotted in Figures 6 and 7.

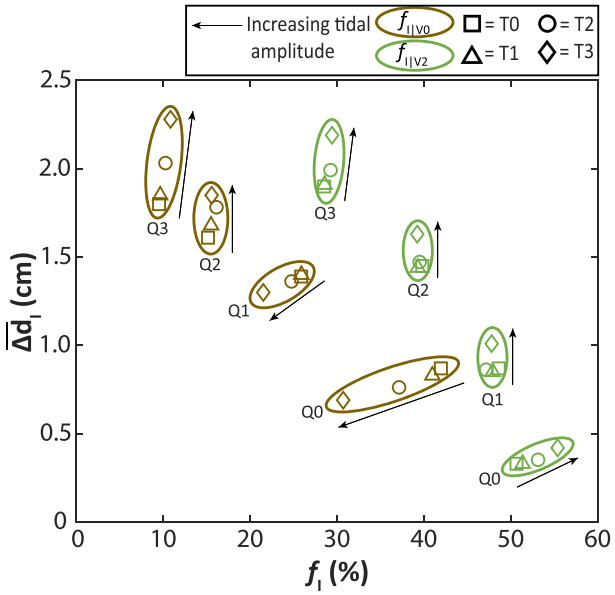

Figure 7. The relationship between sediment retention and accretion at the island-scale. The data groupings are labeled by riverine flood conditions (*Q0–3*) and outlined by solid brown and green lines denoting the *V0* and *V2* runs, respectively. The solid black arrow alongside each f_I grouping highlights the trend of increasing tidal amplitude.

Second, we consider how the proportion of incoming sediment that is deposited on the island changes (F_I). As Q_w increases, F_I decreases, while $\overline{\Delta d}_I$ increases (Figure 6, solid outlines). This is especially true for the *V0* condition. This negative trend is opposite of the positive trend for $F_{I,P}$ and this arises because silt loss increases with higher Q_w (Figure 6, dashed black arrow). Even though $F_{I,P}$ increases at higher Q_w, F_I decreases because sediment bypasses the islands. The data for *V2* show similar behavior, but the silt loss ($F_{I,P}|_{V2} - F_I|_{V2}$) at a given Q is smaller because vegetation increases sediment retention by decreasing sediment advection off the islands. This tendency of vegetation to increase sediment retention is due to vegetation-induced drag on sediment-laden fluid flow that reduces flow velocities and increases deposition, the net result of which we refer to here as the trapping effect.

To consider the trapping effect more directly, we shift our perspective and consider island-scale retention (f_I; equation (5)), which is sediment deposition relative to the sediment flux onto the islands ($Q_{s,I}$) rather than relative to the total sediment entering the deltaic system at the upstream boundary ($Q_{s,o}$). From the perspective of island-scale retention, vegetation increases retention; in Figure 7 the vegetation runs are always to the right of the unvegetated runs (Table 2; $f_I|_{V0}$ is less than $f_I|_{V2}$ across all Q and T conditions). Still, f_I decreases with greater flood-wave magnitude for both *V0* and *V2*, which underscores that while the trapping effect of vegetation, as parameterized here, consistently enhances silt retention on the islands ~15 to 23% (equation (6)), overall efficiency of deposition on the islands decreases as Q_w increases.

4.3. The Role of Tidal Amplitude

As already discussed, each Q_w and vegetation condition cluster contains four points that correspond to different tidal amplitudes (Figures 6 and 7). Tidal amplitude has a smaller influence on silt retention over the entire delta (Figure 5) and within the deltaic islands (Figures 6 and 7), compared to flood-wave magnitude or the presence of vegetation. But, the effect of tidal amplitude is not monotonic; in some cases tides increase retention and in other cases they decrease it.

Regardless of vegetation or flood-wave magnitude, tides increase $F_{I,P}$ by roughly 1 to 3% for *V0* and *V2* conditions (Figure 6). This occurs because greater tidal amplitude increases island inundation and transports more silt onto the islands. However, as tides recede, they also transport suspended silt out of the islands and this effect can offset the increase in $F_{I,P}$. Notice that for most of our runs, greater tidal amplitude results in greater F_I or f_I (Figures 6 and 7). However, for the *V0* condition at *Q0* and*Q1* the opposite is true, and lower tidal amplitude results in greater silt retention (Figures 6 and 7). This reversal never occurs for the *V2* condition.

This reversal does not occur for *V2* because the trapping effect of vegetation limits sediment export from the islands as the tide recedes. At *Q0* the max-amplitude tide with no vegetation present (*T3V0*) results in higher instantaneous net flux compared to the no tide condition (*T0V0*; Figure 8a). However, the *T3* condition also results in periods of negative instantaneous net flux when more silt leaves the islands than enters, whereas when no tide is present (*T0V0*, *T0V2*), the instantaneous net silt flux is always positive (Figure 8a). The cumulative net silt flux shows that the increased flux during high tide does not offset the sediment exported during low tide, and the result is that tides lower the cumulative flux at *Q0* and *V0* conditions (Figure 8b; dashed brown line is below solid brown line). But for the *V2* conditions, the trapping effect of vegetation reduces silt loss from the islands and the benefit of tides outweighs the detriment, creating a small increase in cumulative net flux (Figures 8a and 8b; dashed green line is slightly above the solid green).

At *Q3* however, the enhanced silt delivery to the islands offsets the loss caused by tides, even in the absence of vegetation. The *V0* and *V2* conditions show similar values of net instantaneous flux at high and low tide (Figure 8d). Initially, the cumulative fluxes for all conditions are also similar, but by 60 hr of model runtime

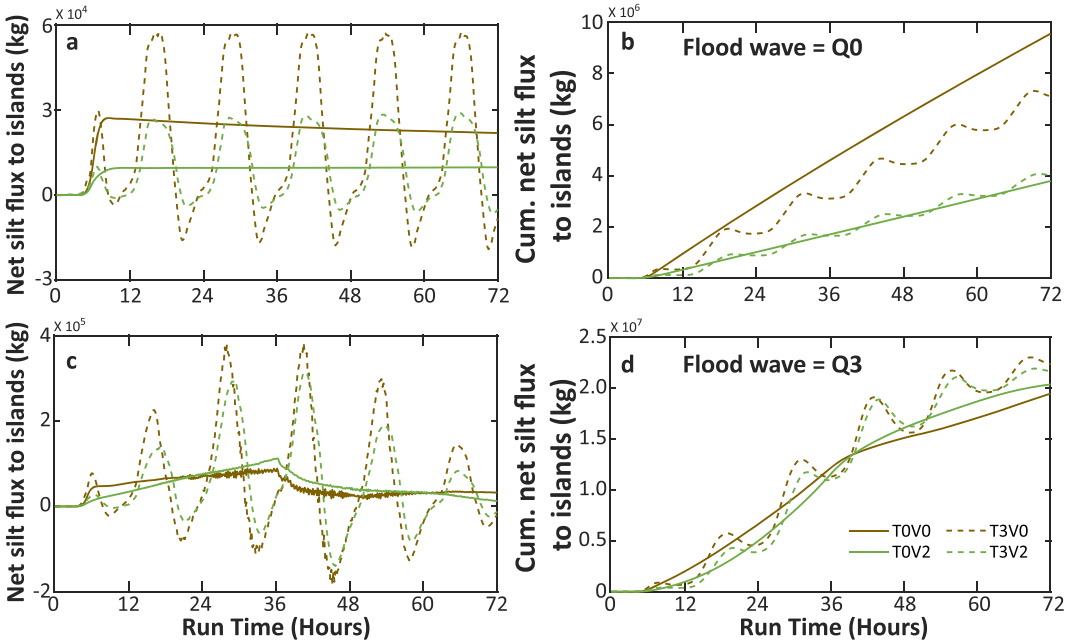

Figure 8. (a and c) Instantaneous net silt flux to all islands over the course of the runs for the null (*T0*; solid) and max tidal amplitude (*T3*; dashed) and for the null (*Q0*) and max riverine flood (*Q3*). Instantaneous net silt flux is the total silt flux into the islands minus the amount that fluxes out of the islands. (b and d) Cumulative net silt flux over the course of the aforementioned runs. Both the unvegetated (*V0*; brown) and vegetated (*V2*; green) conditions for these riverine flood and tidal amplitude end member runs are presented.

the cumulative flux for runs with tides becomes larger than without tides, indicating the net benefit of tides at higher *Q* in the form of increased transport of sediment onto the islands (Figure 8d; dashed brown and green lines are higher than corresponding solid lines at the end of the run).

5. Discussion

5.1. The Competing Effects of Buffering and Trapping Govern How Vegetation Affects Sedimentation

One of the prevailing notions in ecogeomorphology is that, all else being equal, the presence of aboveground vegetation on the marsh surface can enhance sediment deposition by reducing turbulence and flow velocities in the water column, which promotes the settling of sediment out of suspension (Christiansen et al., 2000; Fagherazzi et al., 2012; Kirwan & Murray, 2007; Leonard & Luther, 1995; Morris et al., 2002; Neumeier & Ciavola, 2004). This enhanced sedimentation does not always occur because sparse vegetation can increase turbulence and limit deposition (Larsen, 2019; Temmerman et al., 2007; Yang et al., 2016). Vegetation also reduces bed shear stress thereby limiting remobilization of sediment following initial deposition (Christiansen et al., 2000; Howes et al., 2010; Nepf, 2012a, 2012b). The tendency of vegetation to enhance sedimentation is often formalized as a positive effect (Larsen, 2019), especially in models of salt marshes (Fagherazzi et al., 2012; Kirwan & Murray, 2007, and references therein) and fluvial floodplains (Kleinhans et al., 2018, and references therein), where the presence of vegetation, up to a point, causes faster rates of vertical surface accretion. This positive vegetation-sedimentation effect in our study is manifested as sediment trapping. Another well-documented effect of vegetation is the occurrence of a stress-divergence feedback. As water interacts with an isolated patch of vegetation, the difference of roughness between the vegetation and the smoother bed surrounding it causes stress to diverge and concentrates flow along the patch margins where there is less resistance (Chen et al., 2012; Larsen, 2019; Nepf, 2012a, 2012b; Temmerman et al., 2005, 2007; Weerman et al., 2012; Yamasaki et al., 2019; Zong & Nepf, 2010). This can lead to erosion at the patch margin, further concentration of flow, and eventual channelization. While we did not simulate planform development and channelization in our model, this stress-divergence feedback

is the mechanism in our runs that creates the buffering effect, which reduces sediment transport onto the islands due to the presence of vegetation.

The trapping and buffering effects together determine whether vegetation causes an increase or decrease in sedimentation in a morphodynamic system. An interesting result of our modeling experiments is that for the vegetation conditions we consider, vegetation decreases sedimentation (*V2* clusters always have equal or less $\overline{\Delta d}_I$ than *V0* clusters; Figures 6 and 7). This stands in contrast to previous studies where vegetation causes an increase in sedimentation compared to unvegetated conditions (Fagherazzi et al., 2012; Kirwan & Murray, 2007; Larsen, 2019). This arises in our results because the buffering effect is always larger than the trapping effect for our chosen vegetation height and density conditions. This balancing act between trapping and buffering is not usually considered or parameterized in models. This could be, in part, because many studies on vegetation and sedimentation focus on salt marsh environments (e.g., Fagherazzi et al., 2012, and references therein), where the buffering effect is minimized because sediment and water flow into a closed tidal basin. In closed tidal basins, water and sediment enter and exit through the same cross section, and the presence of vegetation predominately affects the location along the tidal channel network that sediment enters the marsh, but not the total sediment flux onto the marsh surface (Temmerman et al., 2005, 2007). In deltaic marshes, on the other hand, the basin is not closed, and water and sediment can flow onto the marshes, or bypass them completely by flowing through the channel network and into the ocean.

The buffering and trapping effects in our model, for the vegetation characteristics tested, can be tracked in Figure 6 by following the trajectory from $F_{I,P}|_{V0} \rightarrow F_{I,P}|_{V2} \rightarrow F_I|_{V2}$ for any given discharge condition. For example, at *Q1*, $F_{I,P}|_{V2}$is less than $F_{I,P}|_{V0}$ because of the buffering effect (Figure 6, dashed gray arrow). The amount retained on the islands, $F_I|_{V2}$, is lower than the incoming flux $F_{I,P}|_{V2}$ (Figure 6, dashed black arrows) because some silt is lost from the islands. For *Q0*, *Q1*, and *Q2* the combined effects of buffering ($F_{I,P}|_{V0} \rightarrow F_{I,P}|_{V2}$; dashed gray line) and silt loss from the islands ($F_{I,P}|_{V2} \rightarrow F_I|_{V2}$; dashed black arrow) are always larger than the silt loss for unvegetated conditions ($F_{I,P}|_{V0} \rightarrow F_I|_{V0}$; dashed black arrow; Figure 6). Because of this, the *V2* conditions have smaller F_I and $\overline{\Delta d}_I$ than *V0* conditions.

At higher discharges it seems that the trapping effect balances out the buffering effect. At *Q3* for both *V0* and *V2*, F_I and $\overline{\Delta d}_I$ are nearly identical. A reasonable conjecture would then be that at discharges higher than *Q3* vegetation might result in higher retention and more deposition. But, the *Q3* discharge of 8,000 $\mathrm{m}^3\ \mathrm{s}^{-1}$ is nearly the maximum observed through the Wax Lake Outlet and does not recur often, so it seems at river discharges less than *Q3* vegetation will not create higher sedimentation on WLD. However, we only used one set of vegetation characteristics in our runs and the interaction of the buffering and trapping effects should vary as these characteristics change (Nardin et al., 2016; Nardin & Edmonds, 2014). In particular, Nardin and Edmonds (2014) found that silt deposition showed divergent behavior; in some cases vegetation caused more silt deposition, and in other cases it caused less. In explorations of vegetation parameter space Nardin and Edmonds (2014) and Nardin et al. (2016) found that certain vegetation heights and spatial density optimize sediment trapping. With greater vegetation heights and densities, sediment remains in the channels (buffering effect), while shorter, sparse vegetation fails to enhance deposition (weak trapping effect). Given these earlier findings, a next step would be to revisit this parameter space to test the relative effects of trapping and buffering on sediment retention over a range of vegetation heights and densities with our model of WLD.

5.2. Operational Consideration and Trade-Offs for Sediment Diversions

Efforts toward mitigation and reversal of wetland loss in coastal deltaic wetlands, like the MRD, often consider positive vertical accretion as a measure of success. Because vertical accretion is so important for mitigation of deltaic land loss, inorganic sediment is one of the most valuable resources along disappearing coastlines. But, river management structures, like dams and levees, have reduced sediment supply to the coast making it important to achieve vertical accretion of the marsh platform with efficient sediment retention. As one might guess, in river-dominated deltas like the one studied here, big floods lead to significant sediment deposition in the delta and on the islands (Bevington et al., 2017; Carle et al., 2015; Esposito et al., 2013; Kolker et al., 2012; Rosenheim et al., 2013; Shen et al., 2015; Snedden et al., 2007). But, that comes at a trade-off because as vertical accretion goes up, sediment retention goes down (Figures 6 and 7). Fieldwork by Keogh et al. (2019) showed similar results. Thus, while larger riverine floods may enhance vertical accretion of existing deltaic wetlands (a desired outcome of sediment diversion

construction), it comes at the cost of lower sediment retention in the delta, relative to the total volume of incoming sediment.

Based on the fieldwork in the Davis Pond diversion, Keogh et al. (2019) proposed a conceptual model that suggests an optimal discharge range for sediment deposition, beyond which deposition will decrease. Our deposition results for the deltaic islands do not follow this conceptual model because deposition increases monotonically up to the highest-magnitude riverine flood WLD is likely to experience. The inconsistency between our results and the Keogh et al. (2019) conceptual model may be due to the differences in the scales of sediment retention. Our results focus on deposition within the deltaic islands, while Keogh et al. (2019) considered deposition within the entire Davis Pond basin. Additionally, Keogh et al. (2019) developed the conceptual model based on data extrapolated from limited data (average discharges for winter/spring and summer/fall for one year), which lie on the lower end of the discharge range for the diversion. Thus, our results indicate that for the WLD system, within the range of riverine flood magnitudes considered here, higher (*Q3*) rather than intermediate (*Q2*) peak flood discharges should be considered for diversion operations if the goal is to maintain or aggrade existing wetlands.

Timing of operations is another important factor to consider when seeking to maximize land-building potential of a sediment diversion. Peyronnin et al. (2017) suggested operational strategies for the planned Mid-Barataria Sediment Diversion (~45 km downstream of New Orleans, Louisiana on the western side of the Mississippi River) by identifying periods of the annual hydrograph during which diversion operations would maximize land building while seeking to limit detrimental impact to the existing ecosystem. Focusing diversion operations in the winter and/or early spring takes advantage of the higher concentration of sand, silt, and clay typically carried by the first peak of the water year (Allison et al., 2012; Peyronnin et al., 2017). Operations later in the year should seek to operate the diversion on the rising limb of flood peaks in order to capture as much sediment in the diversion as possible, per unit of freshwater entering the diversion (Peyronnin et al., 2017). Additionally, Peyronnin et al. (2017) suggested that winter operation while vegetation is senesced could reduce vegetation stress and loss from prolonged flooding. Our study further supports that operations be focused in the winter/early spring period of the year, because during this period larger magnitude discharges occur and vegetation is senesced; both conditions create greater vertical accretion of existing wetlands (Figures 6 and 7). However, it should be kept in mind, as stated earlier, that maximizing this vertical accretion will come at the cost of a lower proportion of the total of sediment input to the delta being retained due to greater throughput to the basin. While more work is required on the subject, we note the suggestion by Peyronnin et al. (2017) that cold fronts during the winter/spring could help maximize sediment resuspension and transfer back onto wetland surface from the basin, which could help improve sediment retention and further improve vertical accretion.

Finally, while perhaps the smallest influence considered in our study, our results show that tides have an important impact on sediment retention and deposition, even in the face of high discharges (Figures 6 and 7). Consider that at *Q3* for the *V0* condition, the *T3* amplitude results in an ~0.5 cm per 60-day flood increase in $\overline{\Delta d}_I$ compared to *T1*. Thus at higher Q_w, tides enhance deposition with minimal change to retention (Figures 6 and 7). In this way, if diversion operations are timed to coincide with higher spring tides it could create more vertical accretion. Furthermore, larger tidal amplitudes also may help mitigate sediment loss from the deltaic system by reducing higher flood velocities that move sediment into the basin (Wright, 1977). F_{DF} decreases with greater tidal amplitude, suggesting this reducing effect fails to retain more sediment on the distal edge of the delta (Table 1). However, F_B increases, while F_{UD} decreases with greater tidal amplitude, indicating that greater tidal amplitudes may be helping to retain more sediment in the basin adjacent to the delta and possibly contribute to reduced transport of sediment offshore (Table 1). Finer spatial analyses of where within the basin this retained sediment is deposited would help clarify this. It should also be noted that our delineation of the delta front/basin boundary was only one of various possible definitions. A different boundary definition may place the boundary further seaward, resulting in different F_{DF} and F_B trends, and thus points to the need for standardization and wide application of the definition for the delta front/basin boundary in future studies.

5.3. Modeling Study Limitations

While our numerical modeling study provides insight on the general distribution of sediment retention within the Wax Lake Delta and how that distribution varies as a function of changing flood-wave

magnitude, tidal amplitude, and extent of vegetation coverage, there are some important limitations to our results that deserve discussion. Like other recent work (Sendrowski & Passalacqua, 2017; Hiatt & Passalacqua, 2015; Shaw & Mohrig, 2014), we also observed an important tidal effect in the WLD despite its microtidal environment (Figures 6 and 7). For our tidal boundary condition we used a simplified semidiurnal tide, even though tides on WLD are actually mixed semidiurnal. This was done to reduce the number of interacting tidal variables. Because we do not simulate a mixed tide, our model likely overpredicts tidally induced flooding and draining of the delta during part of the tide and thus may be overpredicting tidally induced transport of sediment in and out of the islands. Given the observed potential importance of tides and that they influence sediment retention year round, as opposed to seasonal hydrological and meteorological forces (i.e., floods and cold fronts) and presence of vegetation, an important future avenue of research would be to see how different tidal components impact retention on WLD.

Another limitation of our study is our parameterization of vegetation and the modeling of its influence on flow and sediment transport processes. We simulate a delta with uniform vegetation character and coverage on a 20-m resolution grid, which limits our ability to include the effect of vegetation patches that occurs at smaller scales (Zong & Nepf, 2010; Chen et al., 2012; Follett & Nepf, 2012; Ortiz et al., 2013; Kim et al., 2015). But, we think that patchy vegetation dynamics could play an important role in morphodynamic evolution of WLD. Numerical experiments show that when patches emerge the flow concentrates between them, leading to erosion, and channelization (Yamaski et al., 2019). This patch-scale feedback may strongly influence sediment retention on deltas, like WLD. Consider that the side channels that allow for water and sediment to enter island interiors (Figure 1a, inset) are important for sediment and water exchange between channels and islands and may be the result of patch-scale feedback (Piliouras & Kim, 2019; Wright et al., 2018). Hence, the patch-scale feedback that creates channels and connectivity counterbalances the buffering effect that limits flow onto the islands. Similarly, estimation of sediment transport onto the deltaic islands along patchy interfaces, for example, along the vegetated fringe within the island interiors, may be lower than what occurs in the real world. Future work could build on this study and the previous work of Wright et al. (2018) who modeled the influence of vegetation patchiness on hydrological connectivity between a primary distributary and adjacent deltaic islands by attempting to better emulate this patchy vegetation pattern and assess its influence in the presence of tidally modulated flow conditions within the island interiors.

Finally, we only consider one noncohesive grain size our study (59 μm) and these results should change for sand size particles, which are less readily transported and travel closer to the bed in the water column. For example, Allison et al. (2017) observed greater retention of sand (100 to 40%) than silt (60 to 4%) over the course of their study of the West Bay basin because silt is more easily transported out of system by rising discharge. Thus, the use of only silt in our model likely results in a lower estimation of sediment retention within the delta as a whole (F_{delta}) than if sand had also been included in our model. Additionally, Nardin and Edmonds (2014) found that while vegetation regularly enhanced sedimentation of mud within existing marsh, sedimentation of sand was only enhanced over a limited range of intermediate vegetation height and density, as compared to when vegetation was absent. This was suggested to be the case because intermediate vegetation height and density sufficiently enhances flow velocity within the channels, better enabling sand transport, while still allowing flow of water onto the marsh surface. By comparison, lower and higher vegetation heights and densities result in less sand transport due to insufficient enhancement of flow velocities in the channels or too great a reduction of water flux onto the marsh, respectively. Thus, it is possible that for a certain range of vegetation conditions, the addition of sand to our model could increase sediment retention on the islands (F_{islands}).

6. Conclusions

In this study we used a calibrated numerical model of the WLD, Louisiana to consider how river discharge, tidal amplitude, and vegetation extent influence sediment retention. We used Delft3D to model sediment retention under different combinations of a triangular riverine flood, a semidiurnal tide, and uniformly dense vegetation. The most important factor for sediment retention is river discharge, because that is the primary supplier of sediment. As discharge increases, vertical accretion of existing wetlands increases, but sediment retention, relative to the total incoming flux, across the whole delta decreases from 72 to 34% because more sediment bypasses the delta to the basin. This highlights an important trade-off for sediment-starved

deltas: enhanced rates of vertical accretion come at the expense of retaining a lower proportion of the total incoming sediment flux to the delta.

We find that in all scenarios tested here vegetation results in less vertical accretion of the islands and lower sediment retention than if vegetation is not present. This occurs because of the interaction of the buffering and trapping effects of vegetation. Buffering reduces sediment flux onto islands because water follows the smoother path in the channels, whereas trapping enhances deposition. In our runs the buffering effect is always greater than trapping. But, we modeled only one vegetation condition of uniform height and density, and more study is needed to consider how variations in vegetation height and/or density alter this outcome.

Larger tidal amplitudes increase vertical accretion at higher discharges and they may help to reduce sediment bypass to the basin, although efforts should be made to simulate more accurate mix semidiurnal tides in future investigation of the role of tides. Generally, our findings suggest timing of diversion operations during higher-amplitude tides, in the winter/spring months when discharges are typically higher in the MRD system and vegetation is senesced may maximize vertical accretion of existing wetlands.

Acknowledgments
This work was supported by National Science Foundation grants 1812019, 1426997, and 1135427. All numerical modeling data and setup files are available through the IU ScholarWorks repository at the following URL: http://hdl.handle.net/2022/24968 and DOI: 10.5967/rz7b-qs71. We would like to thank Deon Knights for the assistance with fieldwork and the Coastal Systems Ecology Lab at Louisiana State University for the access to data collected by observation platforms located in the Wax Lake Delta and maintenance of said platforms.

References

Allison, M. A., Demas, C. R., Ebersole, B. A., Kleiss, B. A., Little, C. D., Meselhe, E. A., et al. (2012). A water and sediment budget for the lower Mississippi–Atchafalaya River in flood years 2008–2010: Implications for sediment discharge to the oceans and coastal restoration in Louisiana. *Journal of Hydrology*, *432*, 84–97.

Allison, M. A., Kineke, G. C., Gordon, E. S., & Goni, M. A. (2000). Development and reworking of a seasonal flood deposit on the inner continental shelf off the Atchafalaya River. *Continental Shelf Research*, *20*(16), 2267–2294.

Allison, M. A., Yuill, B. T., Meselhe, E. A., Marsh, J. K., Kolker, A. S., & Ameen, A. D. (2017). Observational and numerical particle tracking to examine sediment dynamics in a Mississippi River delta diversion. *Estuarine, Coastal and Shelf Science*, *194*, 97–108.

Baptist, M. J. (2005). *Modelling floodplain biogeomorphology*. Netherlands: Delft University Press.

Bevington, A. E., Twilley, R. R., Sasser, C. E., & Holm, G. O. Jr. (2017). Contribution of river floods, hurricanes, and cold fronts to elevation change in a deltaic floodplain, northern Gulf of Mexico, USA. *Estuarine, Coastal and Shelf Science*, *191*, 188–200.

Bevington, Azure Elizabeth, Dynamics of land building and ecological succession in a prograding deltaic floodplain, Wax Lake Delta, LA, USA (2016). *LSU Doctoral Dissertations*. 4206. https://digitalcommons.lsu.edu/gradschool_dissertations/4206

Blum, M. D., & Roberts, H. H. (2009). Drowning of the Mississippi Delta due to insufficient sediment supply and global sea-level rise. *Nature Geoscience*, *2*(7), 488.

Cahoon, D. R., White, D. A., & Lynch, J. C. (2011). Sediment infilling and wetland formation dynamics in an active crevasse splay of the Mississippi River delta. *Geomorphology*, *131*(3-4), 57–68.

Carle, M. V., Sasser, C. E., & Roberts, H. H. (2015). Accretion and vegetation community change in the Wax Lake Delta following the historic 2011 Mississippi River flood. *Journal of Coastal Research*, *31*(3), 569–587.

Chen, Z., Ortiz, A., Zong, L., & Nepf, H. (2012). The wake structure behind a porous obstruction and its implications for deposition near a finite patch of emergent vegetation. *Water Resources Research*, *48*. https://doi.org/10.1029/2012WR012224

Childers, D. L., & Day, J. W. (1990). Marsh-water column interactions in two Louisiana estuaries. I. Sediment dynamics. *Estuaries*, *13*(4), 393–403.

Christiansen, T., Wiberg, P. L., & Milligan, T. G. (2000). Flow and sediment transport on a tidal salt marsh surface. *Estuarine, Coastal and Shelf Science*, *50*(3), 315–331.

Couvillion, B. R., Barras, J. A., Steyer, G. D., Sleavin, W., Fischer, M., Beck, H., et al. (2011). Land area change in coastal Louisiana from 1932 to 2010.

CPRA (2017). *Louisiana's Comprehensive Master Plan for a Sustainable Coast* (p. 171). Baton Rouge, LA: Coastal Protection and Restoration Authority of Louisiana.

Day, J., Cable, J., Lane, R., & Kemp, G. (2016). Sediment deposition at the Caernarvon crevasse during the great Mississippi flood of 1927: Implications for coastal restoration. *Water*, *8*(2), 38.

Day, J. W., Agboola, J., Chen, Z., D'Elia, C., Forbes, D. L., Giosan, L., et al. (2016). Approaches to defining deltaic sustainability in the 21st century. *Estuarine, Coastal and Shelf Science*, *183*, 275–291.

Day, J. W., Boesch, D. F., Clairain, E. J., Kemp, G. P., Laska, S. B., Mitsch, W. J., et al. (2007). Restoration of the Mississippi Delta: Lessons from Hurricanes Katrina and Rita. *Science*, *315*(5819), 1679–1684.

Day, J. W., Britsch, L. D., Hawes, S. R., Shaffer, G. P., Reed, D. J., & Cahoon, D. (2000). Pattern and process of land loss in the Mississippi Delta: A spatial and temporal analysis of wetland habitat change. *Estuaries*, *23*(4), 425–438.

Day, J. W., Kemp, G. P., Reed, D. J., Cahoon, D. R., Boumans, R. M., Suhayda, J. M., & Gambrell, R. (2011). Vegetation death and rapid loss of surface elevation in two contrasting Mississippi delta salt marshes: The role of sedimentation, autocompaction and sea-level rise. *Ecological Engineering*, *37*(2), 229–240.

De Lima, P. H., Janzen, J. G., & Nepf, H. M. (2015). Flow patterns around two neighboring patches of emergent vegetation and possible implications for deposition and vegetation growth. *Environmental Fluid Mechanics*, *15*(4), 881–898.

Denes, T. A., & Caffrey, J. M. (1988). Changes in seasonal water transport in a Louisiana estuary, Fourleague Bay, Louisiana. *Estuaries*, *11*(3), 184–191.

Draut, A. E., Kineke, G. C., Huh, O. K., Grymes, J. M. III, Westphal, K. A., & Moeller, C. C. (2005). Coastal mudflat accretion under energetic conditions, Louisiana chenier-plain coast, USA. *Marine Geology*, *214*(1-3), 27–47.

Draut, A. E., Kineke, G. C., Velasco, D. W., Allison, M. A., & Prime, R. J. (2005). Influence of the Atchafalaya River on recent evolution of the chenier-plain inner continental shelf, northern Gulf of Mexico. *Continental Shelf Research*, *25*(1), 91–112.

Esposito, C. R., Georgiou, I. Y., & Kolker, A. S. (2013). Hydrodynamic and geomorphic controls on mouth bar evolution. *Geophysical Research Letters*, *40*, 1540–1545.

Esposito, C. R., Shen, Z., Törnqvist, T. E., Marshak, J., & White, C. (2017). Efficient retention of mud drives land building on the Mississippi Delta plain. *Earth Surface Dynamics*, *5*(3), 387–397.

Fabre, Jeffrey Bryant, Sediment flux & fate for a large-scale diversion: The 2011 Mississippi River Flood, the Bonnet Carré Spillway, and the implications for coastal restoration in south Louisiana (2012). LSU Master's Theses. 931. https://digitalcommons.lsu.edu/gradschool_theses/931

Fagherazzi, S., Kirwan, M. L., Mudd, S. M., Guntenspergen, G. R., Temmerman, S., D'Alpaos, A., et al. (2012). Numerical models of salt marsh evolution: Ecological, geomorphic, and climatic factors. *Reviews of Geophysics*, *50*, RG1002. https://doi.org/10.1029/2011RG000359

Ferguson, R. I., & Church, M. (2004). A simple universal equation for grain settling velocity. *Journal of sedimentary Research*, *74*(6), 933–937.

Follett, E. M., & Nepf, H. M. (2012). Sediment patterns near a model patch of reedy emergent vegetation. *Geomorphology*, *179*, 141–151.

Gagliano, S. M., Meyer-Arendt, K. J., & Wicker, K. M. (1981). Land loss in the Mississippi River deltaic plain. *Trans. Gulf Coast Assoc. Geol. Soc.*, *31*, 295–299.

Gedan, K. B., Kirwan, M. L., Wolanski, E., Barbier, E. B., & Silliman, B. R. (2011). The present and future role of coastal wetland vegetation in protecting shorelines: Answering recent challenges to the paradigm. *Climatic Change*, *106*(1), 7–29.

Geleynse, N., Hiatt, M., Sangireddy, H., & Passalacqua, P. (2015). Identifying environmental controls on the shoreline of a natural river delta. *Journal of Geophysical Research: Earth Surface*, *120*(5), 877–893.

Georgiou, I. Y., FitzGerald, D. M., & Stone, G. W. (2005). The impact of physical processes along the Louisiana coast. *Journal of Coastal Research*, 72–89.

Grace, J. B. (1989). Effects of water depth on *Typha latifolia* and *Typha domingensis*. *American Journal of Botany*, *76*(5), 762–768.

Hiatt, M., Snedden, G., Day, J. W., Rohli, R. V., Nyman, J. A., Lane, R., & Sharp, L. A. (2019). Drivers and impacts of water level fluctuations in the Mississippi River delta: Implications for delta restoration. *Estuarine, Coastal and Shelf Science*, *224*, 117–137.

Hoitink, A. J. F., & Jay, D. A. (2016). Tidal river dynamics: Implications for deltas. *Reviews of Geophysics*, *54*, 240–272. https://doi.org/10.1002/2015RG000507

Howes, N. C., FitzGerald, D. M., Hughes, Z. J., Georgiou, I. Y., Kulp, M. A., Miner, M. D., et al. (2010). Hurricane-induced failure of low salinity wetlands. *Proceedings of the National Academy of Sciences*, *107*(32), 14,014–14,019.

Jankowski, K. L., Törnqvist, T. E., & Fernandes, A. M. (2017). Vulnerability of Louisiana's coastal wetlands to present-day rates of relative sea-level rise. *Nature Communications*, *8*, 14792.

Jaramillo, S., Sheremet, A., Allison, M. A., Reed, A. H., & Holland, K. T. (2009). Wave-mud interactions over the muddy Atchafalaya subaqueous clinoform, Louisiana, United States: Wave-supported sediment transport. *Journal of Geophysical Research*, *114*, C04002. https://doi.org/10.1029/2008JC004821

Kadlec, R. H., & Wallace, S. (2008). *Treatment wetlands*. Boca Raton, FL: CRC Press/Taylor & Francis Group.

Karadogan, E., Willson, C. S., & Berger, C. R. (2009, October). Numerical modeling of the Lower Mississippi River-influence of forcings on flow distribution and impact of sea level rise on the system. In *OCEANS 2009* (pp. 1–7). Biloxi, MS: IEEE.

Keogh, M. E., Kolker, A. S., Snedden, G. A., & Renfro, A. A. (2019). Hydrodynamic controls on sediment retention in an emerging diversion-fed delta. *Geomorphology*, *332*, 100–111.

Kim, H. S., Kimura, I., & Shimizu, Y. (2015). Bed morphological changes around a finite patch of vegetation. *Earth Surface Processes and Landforms*, *40*(3), 375–388.

Kim, W., Mohrig, D., Twilley, R., Paola, C., & Parker, G. (2009). Is it feasible to build new land in the Mississippi River Delta? *Eos, Transactions American Geophysical Union*, *90*(42), 373–374.

Kineke, G. C., Higgins, E. E., Hart, K., & Velasco, D. (2006). Fine-sediment transport associated with cold-front passages on the shallow shelf, Gulf of Mexico. *Continental Shelf Research*, *26*(17-18), 2073–2091.

Kineke, G. C., Sternberg, R. W., Trowbridge, J. H., & Geyer, W. R. (1996). Fluid-mud processes on the Amazon continental shelf. *Continental Shelf Research*, *16*(5-6), 667–696.

Kirwan, M. L., & Murray, A. B. (2007). A coupled geomorphic and ecological model of tidal marsh evolution. *Proceedings of the National Academy of Sciences*, *104*(15), 6118–6122.

Kleinhans, M. G., de Vries, B., Braat, L., & van Oorschot, M. (2018). Living landscapes: Muddy and vegetated floodplain effects on fluvial pattern in an incised river. *Earth Surface Processes and Landforms*, *43*(14), 2948–2963. https://doi.org/10.1002/esp.4437

Kolker, A. S., Allison, M. A., & Hameed, S. (2011). An evaluation of subsidence rates and sea-level variability in the northern Gulf of Mexico. *Geophysical Research Letters*, *38*, L21404. https://doi.org/10.1029/2011GL049458

Kolker, A. S., Miner, M. D., & Weathers, H. D. (2012). Depositional dynamics in a river diversion receiving basin: The case of the West Bay Mississippi River Diversion. *Estuarine, Coastal and Shelf Science*, *106*, 1–12.

Lane, E. M., Restrepo, J. M., & McWilliams, J. C. (2007). Wave–current interaction: A comparison of radiation-stress and vortex-force representations. *Journal of Physical Oceanography*, *37*(5), 1122–1141.

Larsen, L. G. (2019). Multiscale flow-vegetation-sediment feedbacks in low-gradient landscapes. *Geomorphology*.

Leonard, L. A., & Luther, M. E. (1995). Flow hydrodynamics in tidal marsh canopies. *Limnology and Oceanography*, *40*(8), 1474–1484.

Lightbody, A. F., & Nepf, H. M. (2006). Prediction of velocity profiles and longitudinal dispersion in salt marsh vegetation. *Limnology and Oceanography*, *51*(1), 218–228.

Ma, H., Larsen, L. G., & Wagner, R. W. (2018). Ecogeomorphic feedbacks that grow deltas. *Journal of Geophysical Research: Earth Surface*, *123*(12), 3228–3250.

Madden, C. J., Day, J. W. Jr., & Randall, J. M. (1988). Freshwater and marine coupling in estuaries of the Mississippi River deltaic plain 1. *Limnology and Oceanography*, *33*(4part2), 982–1004.

Mariotti, G. (2016). Revisiting salt marsh resilience to sea level rise: Are ponds responsible for permanent land loss? *Journal of Geophysical Research: Earth Surface*, *121*, 1391–1407.

Meade, R. H., & Moody, J. A. (2010). Causes for the decline of suspended-sediment discharge in the Mississippi River system, 1940–2007. *Hydrological Processes: An International Journal*, *24*(1), 35–49.

Meire, D. W., Kondziolka, J. M., & Nepf, H. M. (2014). Interaction between neighboring vegetation patches: Impact on flow and deposition. *Water Resources Research*, *50*, 3809–3825. https://doi.org/10.1002/2013WR015070

Miller, R. L., & Fujii, R. (2010). Plant community, primary productivity, and environmental conditions following wetland re-establishment in the Sacramento-San Joaquin Delta, California. *Wetlands Ecology and Management*, *18*(1), 1–16.

Morris, J. T., Sundareshwar, P. V., Nietch, C. T., Kjerfve, B., & Cahoon, D. R. (2002). Responses of coastal wetlands to rising sea level. *Ecology*, *83*(10), 2869–2877.

Nardin, W., & Edmonds, D. A. (2014). Optimum vegetation height and density for inorganic sedimentation in deltaic marshes. *Nature Geoscience*, *7*(10), 722.
Nardin, W., Edmonds, D. A., & Fagherazzi, S. (2016). Influence of vegetation on spatial patterns of sediment deposition in deltaic islands during flood. *Advances in Water Resources*, *93*, 236–248.
Neill, C. F., & Allison, M. A. (2005). Subaqueous deltaic formation on the Atchafalaya Shelf, Louisiana. *Marine Geology*, *214*(4), 411–430.
Nepf, H. M. (1999). Drag, turbulence, and diffusion in flow through emergent vegetation. *Water Resources Research*, *35*(2), 479–489.
Nepf, H. M. (2012a). Flow and transport in regions with aquatic vegetation. *Annual Review of Fluid Mechanics*, *44*, 123–142.
Nepf, H. M. (2012b). Hydrodynamics of vegetated channels. *Journal of Hydraulic Research*, *50*(3), 262–279.
Neumeier, U., & Ciavola, P. (2004). Flow resistance and associated sedimentary processes in a *Spartina maritima* salt-marsh. *Journal of Coastal Research*, *20*(2), 435–447.
NOAA (2011). *USGS Atchafalaya 2 LiDAR*. Charleston, SC: NOAA's Ocean Service, Office for Coastal Management (OCM).
Olliver, E. A., & Edmonds, D. A. (2017). Defining the ecogeomorphic succession of land building for freshwater, intertidal wetlands in Wax Lake Delta, Louisiana. *Estuarine, Coastal and Shelf Science*, *196*, 45–57.
Ortiz, A. C., Ashton, A., & Nepf, H. (2013). Mean and turbulent velocity fields near rigid and flexible plants and the implications for deposition. *Journal of Geophysical Research: Earth Surface*, *118*, 2585–2599. https://doi.org/10.1002/2013JF002858
Ortiz, A. C., Roy, S., & Edmonds, D. A. (2017). Land loss by pond expansion on the Mississippi River Delta Plain. *Geophysical Research Letters*, *44*, 3635–3642.
Paola, C., Twilley, R. R., Edmonds, D. A., Kim, W., Mohrig, D., Parker, G., et al. (2011). Natural processes in delta restoration: Application to the Mississippi Delta. *Annual Review of Marine Science*, *3*, 67–91. https://doi.org/10.1146/annurev-marine-120709-142856
Partheniades, E. (1965). Erosion and deposition of cohesive soils. *Journal of the Hydraulics Division*, *91*(1), 105–139.
Perez, B. C., Day, J. W. Jr., Rouse, L. J., Shaw, R. F., & Wang, M. (2000). Influence of Atchafalaya River discharge and winter frontal passage on suspended sediment concentration and flux in Fourleague Bay, Louisiana. *Estuarine, Coastal and Shelf Science*, *50*(2), 271–290.
Peyronnin, N., Caffey, R., Cowan, J., Justic, D., Kolker, A., Laska, S., et al. (2017). Optimizing sediment diversion operations: Working group recommendations for integrating complex ecological and social landscape interactions. *Water*, *9*(6), 368.
Piliouras, A., & Kim, W. (2019). Delta size and plant patchiness as controls on channel network organization in experimental deltas. *Earth Surface Processes and Landforms*, *44*(1), 259–272.
Roberts, H. H., Coleman, J. M., Bentley, S. J., & Walker, N. (2003). An embryonic major delta lobe: A new generation of delta studies in the Atchafalaya-Wax Lake Delta system.
Roberts, H. H., Walker, N., Cunningham, R., Kemp, G. P., & Majersky, S. (1997). Evolution of sedimentary architecture and surface morphology: Atchafalaya and Wax Lake Deltas, Louisiana (1973-1994).
Rosen, T., & Xu, Y. J. (2013). Recent decadal growth of the Atchafalaya River Delta complex: Effects of variable riverine sediment input and vegetation succession. *Geomorphology*, *194*, 108–120.
Rosenheim, B. E., Roe, K. M., Roberts, B. J., Kolker, A. S., Allison, M. A., & Johannesson, K. H. (2013). River discharge influences on particulate organic carbon age structure in the Mississippi/Atchafalaya River System. *Global Biogeochemical Cycles*, *27*, 154–166. https://doi.org/10.1002/gbc.20018
Sendrowski, A., & Passalacqua, P. (2017). Process connectivity in a naturally prograding river delta. *Water Resources Research*, *53*, 1841–1863. https://doi.org/10.1002/2016WR019768
Shaw, J. B., Ayoub, F., Jones, C. E., Lamb, M. P., Holt, B., Wagner, R. W., et al. (2016). Airborne radar imaging of subaqueous channel evolution in Wax Lake Delta, Louisiana, USA. *Geophysical Research Letters*, *43*, 5035–5042.
Shaw, J. B., & Mohrig, D. (2014). The importance of erosion in distributary channel network growth, Wax Lake Delta, Louisiana, USA. *Geology*, *42*(1), 31–34.
Shaw, J. B., Mohrig, D., & Whitman, S. K. (2013). The morphology and evolution of channels on the Wax Lake Delta, Louisiana, USA. *Journal of Geophysical Research: Earth Surface*, *118*(3), 1562–1584.
Shen, Z., Törnqvist, T. E., Mauz, B., Chamberlain, E. L., Nijhuis, A. G., & Sandoval, L. (2015). Episodic overbank deposition as a dominant mechanism of floodplain and delta-plain aggradation. *Geology*, *43*(10), 875–878.
Smith, J. E., Bentley, S. J., Snedden, G. A., & White, C. (2015). What role do hurricanes play in sediment delivery to subsiding river deltas? *Scientific Reports*, *5*, 17582.
Snedden, G. A., Cable, J. E., Swarzenski, C., & Swenson, E. (2007). Sediment discharge into a subsiding Louisiana deltaic estuary through a Mississippi River diversion. *Estuarine, Coastal and Shelf Science*, *71*(1-2), 181–193.
Stanley, D. J., & Warne, A. G. (1993). Nile Delta: recent geological evolution and human impact. *Science*, *260*(5108), 628–634. https://doi.org/10.1126/science.260.5108.628
Stern, M. K., Day, J. W., & Teague, K. G. (1991). Nutrient transport in a riverine-influenced, tidal freshwater bayou in Louisiana. *Estuaries*, *14*(4), 382–394.
Stumpf, R. P. (1983). The process of sedimentation on the surface of a salt marsh. *Estuarine, Coastal and Shelf Science*, *17*(5), 495–508.
Syvitski, J. P., & Saito, Y. (2007). Morphodynamics of deltas under the influence of humans. *Global and Planetary Change*, *57*(3-4), 261–282.
Syvitski, J. P., Vörösmarty, C. J., Kettner, A. J., & Green, P. (2005). Impact of humans on the flux of terrestrial sediment to the global coastal ocean. *Science*, *308*(5720), 376–380. https://doi.org/10.1126/science.1109454
Tanino, Y., & Nepf, H. M. (2008). Laboratory investigation of mean drag in a random array of rigid, emergent cylinders. *Journal of Hydraulic Engineering*, *134*(1), 34–41.
Temmerman, S., Bouma, T. J., Govers, G., Wang, Z. B., De Vries, M. B., & Herman, P. M. J. (2005). Impact of vegetation on flow routing and sedimentation patterns: Three-dimensional modeling for a tidal marsh. *Journal of Geophysical Research: Earth Surface*, *110*(F4). https://doi.org/10.1029/2005JF000301
Temmerman, S., Bouma, T. J., Van de Koppel, J., Van der Wal, D., De Vries, M. B., & Herman, P. M. J. (2007). Vegetation causes channel erosion in a tidal landscape. *Geology*, *35*(7), 631–634.
Traykovski, P., Trowbridge, J., & Kineke, G. (2015). Mechanisms of surface wave energy dissipation over a high-concentration sediment suspension. *Journal of Geophysical Research: Oceans*, *120*(3), 1638–1681.
Turner, R. E., Baustian, J. J., Swenson, E. M., & Spicer, J. S. (2006). Wetland sedimentation from Hurricanes Katrina and Rita. *Science*, *314*(5798), 449–452. https://doi.org/10.1126/science.1129116
Van Dijk, W. M., Teske, R., Van de Lageweg, W. I., & Kleinhans, M. G. (2013). Effects of vegetation distribution on experimental river channel dynamics. *Water Resources Research*, *49*(11), 7558–7574.
Van Heerden, I. L., & Roberts, H. H. (1988). Facies development of Atchafalaya Delta, Louisiana: A modern bayhead delta. *AAPG Bulletin*, *72*(4), 439–453.

Vandenbruwaene, W., Temmerman, S., Bouma, T. J., Klaassen, P. C., De Vries, M. B., Callaghan, D. P., et al. (2011). Flow interaction with dynamic vegetation patches: Implications for biogeomorphic evolution of a tidal landscape. *Journal of Geophysical Research*, *116*. https://doi.org/10.1029/2010JF001788

Wang, J., Xu, K., Restreppo, G. A., Bentley, S. J., Meng, X., & Zhang, X. (2018). The coupling of bay hydrodynamics to sediment transport and its implication in micro-tidal wetland sustainability. *Marine Geology*, *405*, 68–76.

Weerman, E. J., Van Belzen, J., Rietkerk, M., Temmerman, S., Kéfi, S., Herman, P. M. J., & de Koppel, J. V. (2012). Changes in diatom patch-size distribution and degradation in a spatially self-organized intertidal mudflat ecosystem. *Ecology*, *93*(3), 608–618. https://doi.org/10.1890/11-0625.1

Wright, K., Hiatt, M., & Passalacqua, P. (2018). Hydrological connectivity in vegetated river deltas: The importance of patchiness below a threshold. *Geophysical Research Letters*, *45*(19), 10–416.

Wright, L. D. (1977). Sediment transport and deposition at river mouths: A synthesis. *Geological Society of America Bulletin*, *88*(6), 857–868.

Wright, L. D., & Coleman, J. M. (1972). River delta morphology: Wave climate and the role of the subaqueous profile. *Science*, *176*(4032), 282–284. https://doi.org/10.1126/science.176.4032.282

Wright, L. D., & Coleman, J. M. (1973). Variations in morphology of major river deltas as functions of ocean wave and river discharge regimes. *AAPG Bulletin*, *57*(2), 370–398.

Xing, F., Syvitski, J. P., Kettner, A. J., Meselhe, E. A., Atkinson, J. H., & Khadka, A. K. (2017). Morphological responses of the Wax Lake Delta, Louisiana, to Hurricanes Rita. *Elementa Science of the Anthropocene*. https://doi.org/10.1525/elementa.125

Xu, K., Bentley, S. J., Day, J. W., & Freeman, A. M. (2019). A review of sediment diversion in the Mississippi River Deltaic Plain. *Estuarine, Coastal and Shelf Science*. https://doi.org/10.1016/j.ecss.2019.05.023

Yamasaki, T. N., de Lima, P. H., Silva, D. F., Cristiane, G. D. A., Janzen, J. G., & Nepf, H. M. (2019). From patch to channel scale: The evolution of emergent vegetation in a channel. *Advances in Water Resources*, *129*, 131–145.

Yang, J. Q., Chung, H., & Nepf, H. M. (2016). The onset of sediment transport in vegetated channels predicted by turbulent kinetic energy. *Geophysical Research Letters*, *43*(21), 11–261.

Yang, S. L., Zhang, J., Zhu, J., Smith, J. P., Dai, S. B., Gao, A., & Li, P. (2005). Impact of dams on Yangtze River sediment supply to the sea and delta intertidal wetland response. *Journal of Geophysical Research: Earth Surface*, *110*(F3).

Zong, L., & Nepf, H. (2010). Flow and deposition in and around a finite patch of vegetation. *Geomorphology*, *116*(3-4), 363–372.

Erratum

In Section 3.4, just below Equation (6), the originally published version of this article incorrectly stated that "enhancement of sediment deposition by vegetation in the case of this study is due to decreased drag on sediment laden flow." Enhancement of sediment deposition is due to increased drag on sediment laden flow. The typographical error has been corrected, and this may be considered the authoritative version of record.